AIP | The Journal of Chemical Physics

Modeling the effects of pH and ionic strength on swelling of polyelectrolyte gels

A. D. Drozdov and J. deClaville Christiansen

Citation: The Journal of Chemical Physics **142**, 114904 (2015); doi: 10.1063/1.4914924
View online: http://dx.doi.org/10.1063/1.4914924
View Table of Contents: http://scitation.aip.org/content/aip/journal/jcp/142/11?ver=pdfcov
Published by the AIP Publishing

Modeling the effects of pH and ionic strength on swelling of polyelectrolyte gels

A. D. Drozdov[1,2,a)] and J. deClaville Christiansen[2]
[1]*Center for Plastics Technology, Danish Technological Institute, Gregersensvej 7, Taastrup 2630, Denmark*
[2]*Department of Mechanical and Manufacturing Engineering, Aalborg University, Fibigerstraede 16, Aalborg 9220, Denmark*

(Received 19 November 2014; accepted 3 March 2015; published online 19 March 2015)

A model is developed for the elastic response of a polyelectrolyte gel under unconstrained and constrained swelling in a water bath with an arbitrary pH, where a monovalent salt is dissolved. A gel is treated as a three-phase medium consisting of an equivalent polymer network, solvent (water), and solute (mobile ions). Transport of solvent and solute is thought of as their diffusion through the network accelerated by an electric field formed by mobile and fixed ions and accompanied by chemical reactions (self-ionization of water molecules, dissociation of functional groups attached to polymer chains, and formation of ion pairs between bound charges and mobile counter-ions). Constitutive equations are derived by means of the free energy imbalance inequality for an arbitrary three-dimensional deformation with finite strains. Adjustable parameters in the governing relations are found by fitting equilibrium swelling diagrams on several hydrogels. The effects of pH, ionic strength of solution, and constraints on equilibrium water uptake are studied numerically. © *2015 AIP Publishing LLC.* [http://dx.doi.org/10.1063/1.4914924]

I. INTRODUCTION

This paper is concerned with constitutive modeling and numerical simulation of the elastic response of polyelectrolyte (PE) gels subjected to swelling in a water bath with various pH at various concentrations of dissolved monovalent salts.

Hydrogels are three-dimensional networks of polymer chains linked by covalent bonds, physical cross-links, hydrogen bonds, van der Waals interactions, and crystallite associations.[1] When a dry gel specimen is immersed into water, it swells retaining structural integrity and ability to withstand large deformations. Stimuli-sensitive gels form an important class of hydrogels whose equilibrium degree of swelling and kinetics of solvent uptake are strongly affected by temperature, pH, ionic strength, electric field, light, and enzymes.[2–4]

In pH-responsive gels, functional groups are attached to main or side chains of the polymer network. When pH of water is altered, some of these groups are ionized. Depending on the charge of bound groups, anionic, cationic, and ampholytic gels are distinguished.[5] This work focuses on water uptake by anionic gels whose functional groups dissociate into positively charged mobile ions and negative bound charges.

Studies on swelling of polyelectrolyte gels have a long history starting in the middle of the past century. They have recently become a focus of attention as these materials demonstrate potential for a wide range of "smart" applications including biomedical devices, drug delivery carriers, scaffolds for tissue engineering, filters and membranes for selective diffusion, sensors for on-line process monitoring, soft actuators, and optical systems.[6–9]

Observations on solvent uptake by neutral and PE gels in deionized water reveal that the latter (i) demonstrate a faster kinetics of swelling, and (ii) their equilibrium degree of swelling exceeds that of neutral gels. A higher rate of solvent transport in PE gels is conventionally explained by electro-osmosis: an electric field formed by mobile ions accelerates their flow, which, in turn, induces an increase in diffusivity of water molecules with which these ions are associated. A higher equilibrium water uptake by PE gels is attributed to two mechanisms: (i) development of ionic pressure (an excess pressure induced by the difference in concentrations of ions inside a specimen and in the surrounding water bath) and (ii) electrostatic repulsion of bound charges. Although there are no doubts regarding the importance of both mechanisms, analysis of equilibrium swelling diagrams is traditionally grounded on the hypothesis that ionic pressure plays the key role while the influence of electrostatic interactions is subordinate.[10] This may be explained by the absence of simple expressions for the energy of electrostatic repulsion to be employed in fitting observations.[11–14]

When a salt is added to a water bath, the equilibrium degree of swelling of a PE gel is strongly (by 2–3 orders of magnitude) reduced. Although the concept of ionic pressure together with the Donnan equilibrium conditions explains qualitatively a decrease in water uptake by PE gels induced by the growth of ionic strength, it fails to predict observations quantitatively.[15] Three additional mechanisms are suggested to ensure agreement with observations:[12] (i) condensation of mobile counter-ions around charged functional groups[16] which results in screening of Coulomb electrostatic forces,[17,18] (ii) binding of mobile counter-ions with bound charges

a)E–mail: add@teknologisk.dk. Telephone: +45 72 20 31 42. Fax: +45 72 20 31 12.

accompanied by formation of electrically neutral complexes (ion-pairs), which leads to a decrease in concentration of charged groups distributed along polymer chains,[18–21] and (iii) evolution of the chemical potential of solvent with concentration of mobile ions that causes an increase in the Flory–Huggins interaction parameter.[22,23]

The objective of this study is twofold: (i) to develop constitutive equations for the elastic behavior of PE gels and diffusion of solvent and solutes under arbitrary three-dimensional deformations accompanied by swelling, and (ii) to apply these relations to the analysis of equilibrium swelling diagrams on PE gels immersed into water baths with various concentrations of salts.

Constitutive modeling and simulation of the mechanical response of pH-sensitive hydrogels under three-dimensional deformations with finite strains have attracted substantial attention in the past decade when it has been confirmed by observations that their equilibrium water uptake is strongly affected by geometrical constraints.[24,25] Coupled equations for the elastic behavior and transport of solvent have recently been derived in Refs. 26–33 for PE gels and in Refs. 34 and 35 for polyampholytic gels. The effect of ionic strength of solution on swelling of pH-responsive gels was analyzed in Refs. 36–39, to mention a few.

The novelty of our model consists in the following. (i) Derivation of constitutive equations for the elastic response of and diffusion of solvent and solutes through a PE gel is grounded on the free energy imbalance inequality, which allows an analog of the Henderson–Hasselbach equation for degree of ionization of chains to be developed within a unified approach. (ii) Ionic pressure and electrostatic repulsion of bound charges are taken into account as basic mechanisms for swelling of a pH-responsive gel. (iii) Attachment of mobile counter-ions to bound charges and formation of electrically neutral ion-pairs are considered as the main mechanism for a decay in degree of swelling with ionic strength of solution. (iv) A PE hydrogel is modeled as a three-phase medium consisting of an equivalent polymer network, solvent, and solutes. Its free energy density equals the sum of the specific free energies of non-interacting constituents, the energy of their interactions, and the energy of an electric field formed by mobile ions and bound charges. (v) The strain energy density of an isotropic polymer network is treated as a function of the principal invariants of the Cauchy–Green tensor for transition from its reference (stress-free) state into the actual state. (vi) The reference state of the equivalent network differs from the initial state of a dry undeformed gel. Evolution of the reference state with time under swelling is driven by changes in degree of ionization of chains.

The exposition is organized as follows. Constitutive equations for a PE gel under an arbitrary three-dimensional deformation accompanied by swelling are developed in Sec. II by means of the free energy imbalance inequality. These relations are simplified in Sec. III for the analysis of observations under unconstrained and constrained swelling. Adjustable parameters in the governing equations are found in Sec. IV by fitting experimental swelling diagrams. Concluding remarks are formulated in Sec. V. Details of derivation are collected in Appendices A and B.

II. CONSTITUTIVE MODEL

A PE gel is treated as a three-phase medium composed of a solid phase (an equivalent polymer network), solvent (water), and solutes (mobile ions). Transport of solvent and solutes is modeled as their diffusion through the equivalent polymer network accompanied by chemical reactions (self-ionization of water molecules and dissociation of functional groups attached to chains) and accelerated by the electric field formed by mobile ions and bound charges.

A. Chemical reactions

Due to self-ionization of water

$$2H_2O \rightleftarrows H_3O^+ + OH^-, \tag{1}$$

it contains positively charged hydronium ions H_3O^+ (hydroxide ions H^+ associated with neutral water molecules) and negatively charged hydroxyl radicals OH^-. Concentrations of positive and negative ions are characterized by

$$pH = -\log[H^+], \qquad pOH = -\log[OH^-], \tag{2}$$

where $\log = \log_{10}$, and $[H^+]$, $[OH^-]$ stand for molar concentrations of H^+, OH^- ions. In thermodynamic equilibrium, pH and pOH obey the equality

$$pH + pOH = pK_w, \tag{3}$$

where K_w denotes water ionization constant and $pK_w = -\log K_w$.

To alter pH of water, hydrochloric acid or sodium hydroxide is conventionally added to the bath. Focusing on water uptake under acidic conditions, we suppose that HCl is immersed which dissociates into H^+ ions (associated with water molecules to form hydronium ions) and Cl^- ions,

$$H_2O + HCl \rightleftarrows H_3O^+ + Cl^-. \tag{4}$$

To change ionic strength of water, a monovalent salt is immersed into the bath whose molar fraction θ lies below its solubility threshold. For definiteness, we presume sodium chloride NaCl to be dissolved and dissociated into Na^+ ions (associated with water molecules) and Cl^- ions,

$$H_2O + NaCl \rightleftarrows Na^+H_2O + Cl^-. \tag{5}$$

Under the assumption that hydrochloric acid and sodium chloride are dissociated entirely in water, reactions (4) and (5) are excluded from the consideration in what follows.

When an anionic PE chain is immersed into the bath with deionized water, some functional groups attached to the chain dissociate, which results in formation of positive mobile ions and negative bound charges. Presuming bound charges to be monovalent, we model the ionization process as dissociation of carboxyl groups,

$$H_2O + COOH \rightleftarrows H_3O^+ + COO^-. \tag{6}$$

Dissociation of functional groups in a water bath with dissolved salt is accompanied by the complexation reaction in which ionized carboxyl groups form ion pairs with sodium cations,

$$Na^+H_2O + COO^- \rightleftarrows Na^+COO^- + H_2O. \tag{7}$$

Denote by n_1, n_2, n_3 the numbers of ionized groups COO^-, non-ionized groups COOH, and groups that form ion pairs Na^+COO^-, respectively, and by $n = n_1 + n_2 + n_3$ the entire number of functional groups per chain. Degree of ionization α is defined as the ratio of the number of charged bound groups to the total number of functional groups per chain,

$$\alpha = \frac{n_1}{n}. \tag{8}$$

Bearing in mind that concentrations of electrically neutral functional groups COOH and Na^+COO^- read

$$\beta_{\rm H} = \frac{n_2}{n}, \qquad \beta_{\rm Na} = \frac{n_3}{n}, \tag{9}$$

we obtain

$$\alpha = 1 - \beta_{\rm H} - \beta_{\rm Na}. \tag{10}$$

Denote by $\bar{c}$, $\bar{c}_{\rm H^+}$, $\bar{c}_{\rm Na^+}$, $\bar{c}_{\rm OH^-}$, $\bar{c}_{\rm Cl^-}$ concentrations (number of species per unit volume) of water molecules, hydroxide ions, sodium cations, hydroxyl radicals, and chloride ions in the bath. Molar fractions of ions are connected with their concentrations by the relations

$$[{\rm H^+}] = \kappa\frac{\bar{c}_{\rm H^+}}{\bar{c}}, \qquad [{\rm OH^-}] = \kappa\frac{\bar{c}_{\rm OH^-}}{\bar{c}}, \qquad [{\rm Cl^-}] = \kappa\frac{\bar{c}_{\rm Cl^-}}{\bar{c}}, \tag{11}$$

where $\kappa = 1000/18$ stands for molarity of water. Keeping in mind that NaCl is entirely dissolved, which means that $[Na^+] = \theta$, we find that

$$\theta = \kappa\frac{\bar{c}_{\rm Na^+}}{\bar{c}}. \tag{12}$$

B. Macro-deformation of a hydrogel

We study swelling of a dry gel specimen immersed into a water bath with a fixed pH. Macro-deformation of a gel coincides with that of an equivalent polymer network. For definiteness, the initial configuration is chosen to coincide with that of the undeformed dry specimen. Transformation of the initial state into the actual state is determined by the deformation gradient $\mathbf{F}$. The Cauchy–Green tensors for macro-deformation read

$$\mathbf{B} = \mathbf{F}\cdot\mathbf{F}^\top, \qquad \mathbf{C} = \mathbf{F}^\top\cdot\mathbf{F}, \tag{13}$$

where the dot stands for inner product and $\top$ denotes transpose.

The volume element in the actual configuration dv is expressed by means of the volume element dV in the initial configuration as

$$dv = J dV, \tag{14}$$

where

$$J = \det\mathbf{F}. \tag{15}$$

The surface element $\mathbf{n}da$ with unit normal $\mathbf{n}$ in the actual configuration is connected with the surface element $\mathbf{N}dA$ with unit normal $\mathbf{N}$ in the initial configuration by the equation

$$\mathbf{n}da = J\mathbf{F}^{-\top}\cdot\mathbf{N}dA = J\mathbf{N}\cdot\mathbf{F}^{-1}dA. \tag{16}$$

Denote by C concentration (number of molecules per unit volume in the initial configuration) of water in the actual state. Disregarding volume changes in a hydrogel driven by the presence of solutes and adopting the molecular incompressibility condition, we write

$$J = 1 + Cv, \tag{17}$$

where v stands for the characteristic volume of a water molecule. Neglecting clustering of water molecules in the bath, we estimate v from the condition

$$\bar{c}v = 1. \tag{18}$$

$C_{\rm H^+}$, $C_{\rm Na^+}$, $C_{\rm OH^-}$, $C_{\rm Cl^-}$ denote concentrations of hydroxide ions H^+, sodium cations Na^+, hydroxyl radicals OH^-, and chloride ions Cl^- in the actual state per unit volume in the initial configuration. According to Eq. (17), concentrations of water molecules and mobile ions per unit volume in the actual configuration are given by

$$c = \frac{C}{J}, \qquad c_{\rm H^+} = \frac{C_{\rm H^+}}{J}, \qquad c_{\rm Na^+} = \frac{C_{\rm Na^+}}{J}, \qquad c_{\rm OH^-} = \frac{C_{\rm OH^-}}{J}, \qquad c_{\rm Cl^-} = \frac{C_{\rm Cl^-}}{J}. \tag{19}$$

M denotes the number of chains in the equivalent polymer network per unit volume in the initial configuration. Denote by $C_{\rm b} = Mn$ concentration of functional groups attached to chains, and by $C_{\rm b^-} = Mn_1$ concentration of charged bound groups per unit volume in the initial configuration. It follows from Eqs. (8) and (10) that

$$C_{\rm b^-} = (1 - \beta_{\rm H} - \beta_{\rm Na})C_{\rm b}. \tag{20}$$

C. Electric field

Transport of mobile ions and deformation of polymer chains with charged groups result in formation of an electric field with electrostatic potential Φ. The electric field vectors, $\mathbf{e}$ and $\mathbf{E}$, in the actual and initial states are defined as

$$\mathbf{e} = -\boldsymbol{\nabla}\Phi, \qquad \mathbf{E} = -\boldsymbol{\nabla}_0\Phi, \tag{21}$$

where $\boldsymbol{\nabla}$, $\boldsymbol{\nabla}_0$ are the gradient operators in the actual and initial configurations. A gel is modeled as a linear dielectric material whose electric displacement vector in the actual state reads

$$\mathbf{h} = \epsilon\mathbf{e}, \tag{22}$$

where electric permittivity ϵ is assumed to be constant. It follows from Eqs. (21) and (22), and the chain rule for differentiation

$$\boldsymbol{\nabla}_0\Phi = \boldsymbol{\nabla}\Phi\cdot\mathbf{F} = \mathbf{F}^\top\cdot\boldsymbol{\nabla}\Phi \tag{23}$$

that

$$\mathbf{E} = \mathbf{e}\cdot\mathbf{F} = \mathbf{F}^\top\cdot\mathbf{e}, \qquad \mathbf{h} = \epsilon\mathbf{E}\cdot\mathbf{F}^{-1} = \epsilon\mathbf{F}^{-\top}\cdot\mathbf{E}. \tag{24}$$

Let Ω be an arbitrary domain with boundary $\partial\Omega$ in the initial state. Their images upon transition into the actual configuration are denoted as ω and $\partial\omega$. The Gauss law for a dielectric medium states that the flux of the electric displacement through a closed surface equals the sum of charges enclosed by this surface,

$$\int_{\partial\omega}\mathbf{h}\cdot\mathbf{n}da = \int_\omega r dv,$$

where r stands for charge density in the actual state. It follows from this relation and Eqs. (14) and (16) that

$$\int_{\partial\Omega} J\mathbf{h}\cdot\mathbf{F}^{-\top}\cdot\mathbf{N}\mathrm{d}A=\int_{\Omega} R\mathrm{d}V, \tag{25}$$

where charge density in the initial state $R=rJ$ is given by

$$R=e\Big[C_{\mathrm{H}^+}+C_{\mathrm{Na}^+}-C_{\mathrm{OH}^-}-C_{\mathrm{Cl}^-}-(1-\beta_{\mathrm{H}}-\beta_{\mathrm{Na}})C_{\mathrm{b}}\Big], \tag{26}$$

and e stands for the charge of electron. Applying the Stokes formula to Eq. (25) and introducing the nominal electric displacement

$$\mathbf{H}=J\mathbf{F}^{-1}\cdot\mathbf{h}=J\mathbf{h}\cdot\mathbf{F}^{-\top}, \tag{27}$$

we arrive at the equation

$$\nabla_0\cdot\mathbf{H}=R. \tag{28}$$

It follows from Eqs. (13), (24), and (27) that

$$\mathbf{H}=\epsilon J\mathbf{C}^{-1}\cdot\mathbf{E}=\epsilon J\mathbf{E}\cdot\mathbf{C}^{-1}. \tag{29}$$

Insertion of Eqs. (20), (26), and (29) into Eq. (28) results in the Poisson equation

$$\nabla_0\cdot(\epsilon J\mathbf{C}^{-1}\cdot\nabla_0\Phi)=-e\Big[C_{\mathrm{H}^+}+C_{\mathrm{Na}^+}-C_{\mathrm{OH}^-}-C_{\mathrm{Cl}^-}-(1-\beta_{\mathrm{H}}-\beta_{\mathrm{Na}})C_{\mathrm{b}}\Big]. \tag{30}$$

For an ideal dielectric occupying a domain Ω in the initial configuration, the energy of the electric field reads[40]

$$\int_{\omega}\frac{\mathbf{h}\cdot\mathbf{h}}{2\epsilon}\mathrm{d}v=\int_{\Omega}\frac{1}{2\epsilon J}\mathbf{H}\cdot\mathbf{C}\cdot\mathbf{H}\mathrm{d}V,$$

which implies that the energy density of the electric field per unit volume in the initial configuration is given by

$$W_{\mathrm{el}}=\frac{1}{2\epsilon J}\mathbf{H}\cdot\mathbf{C}\cdot\mathbf{H}. \tag{31}$$

The work of the electric field (per unit time) is determined by the formula[40]

$$\mathcal{U}_{\mathrm{el}}=-\int_{\partial\Omega}\Phi\dot{\mathbf{H}}\cdot\mathbf{N}\mathrm{d}A,$$

where the superscript dot stands for the derivative with respect to time. Transforming the integral by means of the Stokes formula and using Eqs. (21) and (28), we find that

$$\mathcal{U}_{\mathrm{el}}=\int_{\Omega}(\mathbf{E}\cdot\dot{\mathbf{H}}-\Phi\dot{R})\mathrm{d}V.$$

Substitution of Eq. (26) into this relation implies that the work performed by the electric field (per unit volume in the initial configuration and per unit time) reads

$$u_{\mathrm{el}}=\mathbf{E}\cdot\dot{\mathbf{H}}-e\Phi\Big[\dot{C}_{\mathrm{H}^+}+\dot{C}_{\mathrm{Na}^+}-\dot{C}_{\mathrm{OH}^-}-\dot{C}_{\mathrm{Cl}^-}+(\dot{\beta}_{\mathrm{H}}+\dot{\beta}_{\mathrm{Na}})C_{\mathrm{b}}\Big]. \tag{32}$$

D. Kinetic relations

Denote by $\mathbf{J}$, $\mathbf{J}_{\mathrm{H}^+}$, $\mathbf{J}_{\mathrm{Na}^+}$, $\mathbf{J}_{\mathrm{OH}^-}$, $\mathbf{J}_{\mathrm{Cl}^-}$ the flux vectors for water molecules and mobile ions in the initial configuration (numbers of species moving through the unit area per unit time). Their counterparts in the actual configuration read $\mathbf{j}$, $\mathbf{j}_{\mathrm{H}^+}$, $\mathbf{j}_{\mathrm{Na}^+}$, $\mathbf{j}_{\mathrm{OH}^-}$, $\mathbf{j}_{\mathrm{Cl}^-}$. Keeping in mind that $\mathbf{n}\cdot\mathbf{j}\mathrm{d}a=\mathbf{N}\cdot\mathbf{J}\mathrm{d}A$, we find from Eq. (16) that

$$\mathbf{J}=J\mathbf{F}^{-1}\cdot\mathbf{j},\quad \mathbf{J}_{\mathrm{H}^+}=J\mathbf{F}^{-1}\cdot\mathbf{j}_{\mathrm{H}^+},\quad \mathbf{J}_{\mathrm{Na}^+}=J\mathbf{F}^{-1}\cdot\mathbf{j}_{\mathrm{Na}^+},\quad \mathbf{J}_{\mathrm{OH}^-}=J\mathbf{F}^{-1}\cdot\mathbf{j}_{\mathrm{OH}^-},\quad \mathbf{J}_{\mathrm{Cl}^-}=J\mathbf{F}^{-1}\cdot\mathbf{j}_{\mathrm{Cl}^-}. \tag{33}$$

The flux of water in the actual configuration is given by

$$\mathbf{j}=-\frac{Dc}{k_{\mathrm{B}}T}\nabla\mu, \tag{34}$$

where T is the absolute temperature, k_{B} is Boltzmann's constant, D stands for the diffusivity, and μ is chemical potential of water molecules in the gel. It follows from Eqs. (23), (33), and (34) that

$$\mathbf{J}=-\frac{DC}{k_BT}\mathbf{F}^{-1}\cdot\nabla_0\mu\cdot\mathbf{F}^{-1}. \tag{35}$$

The mass conservation law for solvent reads

$$\dot{C}=-\nabla_0\cdot\mathbf{J}+\Gamma, \tag{36}$$

where Γ is the rate of production of water molecules (per unit volume in the initial configuration and unit time) due to self-ionization reaction (1). Combination of Eqs. (35) and (36) yields

$$\dot{C}=\nabla_0\cdot\Big(\frac{DC}{k_BT}\mathbf{F}^{-1}\cdot\nabla_0\mu\cdot\mathbf{F}^{-1}\Big)+\Gamma. \tag{37}$$

Denote by μ_{H^+}, μ_{Na^+}, μ_{OH^-}, μ_{Cl^-} chemical potentials of mobile ions. Their flux vectors in the actual state are determined by analogy with Eq. (35),

$$\mathbf{j}_{\mathrm{H}^+}=-\frac{D_{\mathrm{H}^+}c_{\mathrm{H}^+}}{k_{\mathrm{B}}T}\nabla\mu_{\mathrm{H}^+},\quad \mathbf{j}_{\mathrm{Na}^+}=-\frac{D_{\mathrm{Na}^+}c_{\mathrm{Na}^+}}{k_{\mathrm{B}}T}\nabla\mu_{\mathrm{Na}^+},\quad \mathbf{j}_{\mathrm{OH}^-}=-\frac{D_{\mathrm{OH}^-}c_{\mathrm{OH}^-}}{k_{\mathrm{B}}T}\nabla\mu_{\mathrm{OH}^-},\quad \mathbf{j}_{\mathrm{Cl}^-}=-\frac{D_{\mathrm{Cl}^-}c_{\mathrm{Cl}^-}}{k_{\mathrm{B}}T}\nabla\mu_{\mathrm{Cl}^-}, \tag{38}$$

where D_{H^+}, D_{Na^+}, D_{OH^-}, D_{Cl^-} stand for the corresponding diffusivities. The flux vectors in the initial state read

$$\begin{aligned}\mathbf{J}_{\mathrm{H}^+}&=-\frac{D_{\mathrm{H}^+}C_{\mathrm{H}^+}}{k_{\mathrm{B}}T}\mathbf{F}^{-1}\cdot\nabla\mu_{\mathrm{H}^+}\cdot\mathbf{F}^{-1},\\ \mathbf{J}_{\mathrm{Na}^+}&=-\frac{D_{\mathrm{Na}^+}C_{\mathrm{Na}^+}}{k_{\mathrm{B}}T}\mathbf{F}^{-1}\cdot\nabla\mu_{\mathrm{Na}^+}\cdot\mathbf{F}^{-1},\\ \mathbf{J}_{\mathrm{OH}^-}&=-\frac{D_{\mathrm{OH}^-}C_{\mathrm{OH}^-}}{k_{\mathrm{B}}T}\mathbf{F}^{-1}\cdot\nabla\mu_{\mathrm{OH}^-}\cdot\mathbf{F}^{-1},\\ \mathbf{J}_{\mathrm{Cl}^-}&=-\frac{D_{\mathrm{Cl}^-}C_{\mathrm{Cl}^-}}{k_{\mathrm{B}}T}\mathbf{F}^{-1}\cdot\nabla\mu_{\mathrm{Cl}^-}\cdot\mathbf{F}^{-1}.\end{aligned} \tag{39}$$

Insertion of Eq. (39) into the mass conservation laws for mobile ions

$$\dot{C}_{\mathrm{H}^+}=-\nabla_0\cdot\mathbf{J}_{\mathrm{H}^+}+\Gamma_{\mathrm{H}^+},\quad \dot{C}_{\mathrm{Na}^+}=-\nabla_0\cdot\mathbf{J}_{\mathrm{Na}^+}+\Gamma_{\mathrm{Na}^+},\quad \dot{C}_{\mathrm{OH}^-}=-\nabla_0\cdot\mathbf{J}_{\mathrm{OH}^-}+\Gamma_{\mathrm{OH}^-},\quad \dot{C}_{\mathrm{Cl}^-}=-\nabla_0\cdot\mathbf{J}_{\mathrm{Cl}^-} \tag{40}$$

implies that

$$\begin{aligned}
\dot{C}_{H^+} &= \nabla_0 \cdot \Big(\frac{D_{H^+}C_{H^+}}{k_BT}\mathbf{F}^{-1}\cdot\nabla_0\mu_{H^+}\cdot\mathbf{F}^{-1}\Big) + \Gamma_{H^+},\\
\dot{C}_{Na^+} &= \nabla_0 \cdot \Big(\frac{D_{Na^+}C_{Na^+}}{k_BT}\mathbf{F}^{-1}\cdot\nabla_0\mu_{Na^+}\cdot\mathbf{F}^{-1}\Big) + \Gamma_{Na^+},\\
\dot{C}_{OH^-} &= \nabla_0 \cdot \Big(\frac{D_{OH^-}C_{OH^-}}{k_BT}\mathbf{F}^{-1}\cdot\nabla_0\mu_{OH^-}\cdot\mathbf{F}^{-1}\Big) + \Gamma_{OH^-},\\
\dot{C}_{Cl^-} &= \nabla_0 \cdot \Big(\frac{D_{Cl^-}C_{Cl^-}}{k_BT}\mathbf{F}^{-1}\cdot\nabla_0\mu_{Cl^-}\cdot\mathbf{F}^{-1}\Big).
\end{aligned} \tag{41}$$

Here, Γ_{OH^-} is the rate of production of hydroxyl ions OH^- driven by ionization of water, Γ_{H^+} is the rate of production of hydroxide ions H^+ caused by ionization of water and dissociation of functional groups, and Γ_{Na^+} is the rate of production of sodium ions Na^+ caused by dissociation of ion pairs. It follows from Eqs. (1), (6), and (7) that

$$\begin{aligned}
\Gamma &= 2\Gamma_0, \qquad \Gamma_{H^+} = -\Gamma_0 - \dot{\beta}_H C_b,\\
\Gamma_{OH^-} &= -\Gamma_0, \qquad \Gamma_{Na^+} = -\dot{\beta}_{Na} C_b,
\end{aligned} \tag{42}$$

where Γ_0 is the rate of association of H^+ and OH^- ions in the self-ionization reaction (per unit volume in the initial configuration), $-\dot{\beta}_H C_b$ is the rate of production of H^+ ions driven by dissociation of carboxyl groups COOH, and $-\dot{\beta}_{Na} C_b$ is the rate of production of Na^+ ions caused by dissociation of bound ion pairs Na^+COO^-.

For an arbitrary domain Ω with boundary $\partial\Omega$, the work produced by transport of solvent and solutes per unit time reads[40]

$$\begin{aligned}
\mathcal{U}_{dif} = -\int_{\partial\Omega} &(\mu\mathbf{J} + \mu_{H^+}\mathbf{J}_{H^+} + \mu_{Na^+}\mathbf{J}_{Na^+} + \mu_{OH^-}\mathbf{J}_{OH^-}\\
&+ \mu_{Cl^-}\mathbf{J}_{Cl^-})\cdot\mathbf{N}dA.
\end{aligned}$$

Transforming the integral by means of the Stokes formula and using Eqs. (36) and (40), we find that

$$\begin{aligned}
\mathcal{U}_{dif} = -\int_{\Omega} &(\mathbf{J}\cdot\nabla_0\mu + \mathbf{J}_{H^+}\cdot\nabla_0\mu_{H^+} + \mathbf{J}_{Na^+}\cdot\nabla_0\mu_{Na^+}\\
&+ \mathbf{J}_{OH^-}\cdot\nabla_0\mu_{OH^-} + \mathbf{J}_{Cl^-}\cdot\nabla_0\mu_{Cl^-})dV\\
+ \int_{\Omega}\Big[&\mu(\dot{C}-\Gamma) + \mu_{H^+}(\dot{C}_{H^+}-\Gamma_{H^+})\\
&+ \mu_{Na^+}(\dot{C}_{Na^+}-\Gamma_{Na^+}) + \mu_{OH^-}(\dot{C}_{OH^-}-\Gamma_{OH^-})\\
&+ \mu_{Cl^-}\dot{C}_{Cl^-}\Big]dV.
\end{aligned}$$

It follows from this equality and Eqs. (35) and (39) that the work produced by transport of solvent and solutes (per unit volume in the initial state and unit time) is given by

$$\begin{aligned}
u_{dif} = &\mu(\dot{C}-\Gamma) + \mu_{H^+}(\dot{C}_{H^+}-\Gamma_{H^+}) + \mu_{Na^+}(\dot{C}_{Na^+}-\Gamma_{Na^+})\\
&+ \mu_{OH^-}(\dot{C}_{OH^-}-\Gamma_{OH^-}) + \mu_{Cl^-}\dot{C}_{Cl^-} + \bar{u}_{dif},
\end{aligned} \tag{43}$$

where

$$\bar{u}_{dif} \geq 0. \tag{44}$$

E. Kinematic relations

The reference configuration of the equivalent polymer network (in which stresses in chains vanish) differs from the initial configuration. Transformation from the initial state into the reference state is described by the deformation gradient $\mathbf{f}$. This transformation is induced by (i) transport of water molecules and mobile ions and (ii) ionization of functional groups attached to polymer chains. For an isotropic polymer network, tensor $\mathbf{f}$ reads

$$\mathbf{f} = f^{\frac{1}{3}}\mathbf{I}, \tag{45}$$

where f stands for the coefficient of volume expansion and $\mathbf{I}$ is the unit tensor.

The deformation gradient for elastic deformation $\mathbf{F}_e$ describes transformation of the reference configuration into the actual configuration. This tensor is connected with the deformation gradient for macro-deformation $\mathbf{F}$ by the multiplicative decomposition formula

$$\mathbf{F} = \mathbf{F}_e\cdot\mathbf{f}. \tag{46}$$

Substitution of Eq. (45) into Eq. (46) implies that

$$\mathbf{F} = f^{\frac{1}{3}}\mathbf{F}_e. \tag{47}$$

Differentiation of Eq. (47) with respect to time results in

$$\mathbf{D} = \mathbf{D}_e + \frac{\dot{f}}{3f}\mathbf{I}, \tag{48}$$

where

$$\mathbf{L} = \dot{\mathbf{F}}\cdot\mathbf{F}^{-1}, \qquad \mathbf{L}_e = \dot{\mathbf{F}}_e\cdot\mathbf{F}_e^{-1} \tag{49}$$

stand for the velocity gradients, and

$$\mathbf{D} = \frac{1}{2}(\mathbf{L}+\mathbf{L}^\top), \qquad \mathbf{D}_e = \frac{1}{2}(\mathbf{L}_e+\mathbf{L}_e^\top) \tag{50}$$

denote the rate-of-strain tensors.

The Cauchy–Green tensors for elastic deformation are given by

$$\mathbf{B}_e = \mathbf{F}_e\cdot\mathbf{F}_e^\top, \qquad \mathbf{C}_e = \mathbf{F}_e^\top\cdot\mathbf{F}_e. \tag{51}$$

The derivatives of the principal invariants J_{e1}, J_{e2}, J_{e3} of these tensors with respect to time read

$$\begin{aligned}
\dot{J}_{e1} = 2\mathbf{B}_e:\mathbf{D}_e, \quad \dot{J}_{e2} = 2(J_{e2}\mathbf{I} - J_{e3}\mathbf{B}_e^{-1}):\mathbf{D}_e,\\
\dot{J}_{e3} = 2J_{e3}\mathbf{I}:\mathbf{D}_e,
\end{aligned}$$

where the colon stands for convolution of tensors. Insertion of Eq. (48) into these relations implies that

$$\begin{aligned}
\dot{J}_{e1} &= 2\mathbf{B}_e:\mathbf{D} - \frac{2\dot{f}}{3f}J_{e1},\\
\dot{J}_{e2} &= -2\mathbf{B}_e^{-1}:\mathbf{D}J_{e3} + 2\Big(\mathbf{I}:\mathbf{D} - \frac{2\dot{f}}{3f}\Big)J_{e2},\\
\dot{J}_{e3} &= 2\Big(\mathbf{I}:\mathbf{D} - \frac{\dot{f}}{f}\Big)J_{e3}.
\end{aligned} \tag{52}$$

F. Free energy density

Denote by Ψ the Helmholtz free energy of a gel per unit volume in the initial configuration. The free energy of a gel (treated as a three-phase composite) equals the sum of six components: (i) the energy of solvent and solutes not interacting with each other and with the solid phase Ψ_1, (ii) the energy of the solid phase not interacting with solvent and solutes Ψ_2, (iii) the energy of mixing of the solid phase and

water Ψ_3, (iv) the energy of mixing of water and mobile ions Ψ_4, (v) the energy of mixing of charged and non-charged functional groups attached to polymer chains Ψ_5, and (vi) energy (31) of the electric field formed by mobile ions and bound charges,

$$\Psi = \Psi_1 + \Psi_2 + \Psi_3 + \Psi_4 + \Psi_5 + W_{el}. \tag{53}$$

The specific energy density Ψ_1 reads

$$\Psi_1 = \mu^0 C + \mu^0_{H^+} C_{H^+} + \mu^0_{Na^+} C_{Na^+} + \mu^0_{OH^-} C_{OH^-} + \mu^0_{Cl^-} C_{Cl^-}, \tag{54}$$

where μ^0, $\mu^0_{H^+}$, $\mu^0_{Na^+}$, $\mu^0_{OH^-}$, $\mu^0_{Cl^-}$ denote chemical potentials of non-interacting water molecules and mobile ions.

The free energy density of the polymer network not interacting with solvent and solutes reads

$$\Psi_2 = W(J_{e1}, J_{e2}, J_{e3}, \alpha, f), \tag{55}$$

where W is the sum of the specific mechanical energy stored in chains and the energy of electrostatic interaction of bound charges. This quantity is treated as a function of the principal invariants of the Cauchy–Green tensor for elastic deformation (in accord with the conventional approach in elasto-plasticity), degree of ionization of chains α (the energy of repulsion of ionized functional groups is proportional to this parameter), and coefficient of volume expansion of the network f (the energy of Coulomb forces between bound charges depends on the principal invariants of the Cauchy–Green tensor for macro-deformation J_m which are expressed in terms of J_{em} and f as $J_1 = f^{\frac{2}{3}} J_{e1}$, $J_2 = f^{\frac{4}{3}} J_{e2}$, $J_3 = f^2 J_{e3}$).

With reference to the Flory–Huggins theory, the specific energy of mixing of water molecules and segments of chains is determined by the formula

$$\frac{\Psi_3}{J} = \frac{k_B T}{v}(\phi_f \ln \phi_f + \chi \phi_s \phi_f),$$

where

$$\phi_s = \frac{1}{1 + Cv}, \qquad \phi_f = \frac{Cv}{1 + Cv}$$

denote volume fractions of solid and fluid phases and χ stands for the Flory–Huggins interaction parameter. It follows from these relations and Eq. (17) that

$$\Psi_3 = k_B T C \Big(\ln \frac{Cv}{1 + Cv} + \frac{\chi}{1 + Cv} \Big). \tag{56}$$

For a dilute solution of mobile ions in water, the specific energy of mixing reads

$$\Psi_4 = k_B T \Big[C_{H^+} \Big(\ln \frac{C_{H^+}}{C} - 1 \Big) + C_{Na^+} \Big(\ln \frac{C_{Na^+}}{C} - 1 \Big) + C_{OH^-} \Big(\ln \frac{C_{OH^-}}{C} - 1 \Big) + C_{Cl^-} \Big(\ln \frac{C_{Cl^-}}{C} - 1 \Big) \Big]. \tag{57}$$

The specific energy of mixing of ionized and non-ionized functional gropus is calculated by the conventional formula

$$\Psi_5 = k_B T C_b \Big[\beta_H \ln \beta_H + \beta_A \ln \beta_A + (1 - \beta_H - \beta_A) \ln (1 - \beta_H - \beta_A) \Big]. \tag{58}$$

G. Free energy imbalance inequality

Governing equations for the mechanical response of a gel under isothermal deformation with finite strains are derived by means of the free energy imbalance inequality

$$\dot{\Psi} - u_{mech} - u_{el} - u_{dif} - u_{dis} \le 0, \tag{59}$$

where u_{mech}, u_{el}, u_{dif}, u_{dis} denote works (per unit volume in the initial state and unit time) produced by stresses, electric field, transport of solvent and solutes, and due to dissociation of functional groups and formation of ion pairs. The mechanical work is determined by the conventional formula

$$u_{mech} = J\mathbf{T} : \mathbf{D}, \tag{60}$$

where $\mathbf{T}$ is the Cauchy stress tensor. The works performed by the electric field and induced by diffusion of solvent and solutes are given by Eqs. (32) and (43). The work induced by dissociation of functional groups and formation of ion pairs reads

$$u_{dis} = -(\Delta\mu_H \dot{\beta}_H + \Delta\mu_{Na} \dot{\beta}_{Na}) C_b, \tag{61}$$

where the constants $\Delta\mu_H$, $\Delta\mu_{Na}$ stand for the differences between chemical potentials of ionized functional groups and ion pairs formed by carboxyl groups COO^- with H^+ and Na^+ ions.

Equation (59) is satisfied when functions C and $\mathbf{F}$ are connected by molecular incompressibility condition (17). To account for the latter dependence, we differentiate Eq. (17) with respect to time, use Eq. (A6), and find that

$$\dot{C}v - J\mathbf{I} : \mathbf{D} = 0.$$

Multiplying this equality by an arbitrary function Π and summing the result with Eq. (59), we obtain

$$\dot{\Psi} + \Pi(\dot{C}v - J\mathbf{I} : \mathbf{D}) - u_{mech} - u_{el} - u_{dif} - u_{dis} \le 0. \tag{62}$$

Differentiation of Eq. (53) with respect to time implies that (Appendix A)

$$\dot{\Psi} = 2(\mathbf{K}_{mech} + \mathbf{K}_{el}) : \mathbf{D} + \mathbf{E} \cdot \dot{\mathbf{H}} + \Big[W_{,\alpha} \dot{\alpha} - \Big(\frac{2K}{3f} - W_{,f} \Big) \dot{f} \Big] + \Theta_C \dot{C} + \Theta_{H^+} \dot{C}_{H^+} + \Theta_{Na^+} \dot{C}_{Na^+} + \Theta_{OH^-} \dot{C}_{OH^-} + \Theta_{Cl^-} \dot{C}_{Cl^-} + \Theta_{\beta_H} \dot{\beta}_H + \Theta_{\beta_{Na}} \dot{\beta}_{Na}, \tag{63}$$

where the coefficients are given by Eqs. (A3), (A9), and (A10). Substitution of Eqs. (32), (42), (43), (60), (61), and (63) into Eq. (62) yields

$$\begin{aligned} &[2(\mathbf{K}_{mech} + \mathbf{K}_{pol}) - J(\mathbf{T} + \Pi\mathbf{I})] : \mathbf{D} \\ &+ \Big[W_{,\alpha} \dot{\alpha} - \Big(\frac{2K}{3f} - W_{,f} \Big) \dot{f} \Big] + (\Theta_C + \Pi v - \mu) \dot{C} \\ &+ (\Theta_{H^+} + e\Phi - \mu_{H^+}) \dot{C}_{H^+} + (\Theta_{Na^+} + e\Phi - \mu_{Na^+}) \dot{C}_{Na^+} \\ &+ (\Theta_{OH^-} - e\Phi - \mu_{OH^-}) \dot{C}_{OH^-} + (\Theta_{Cl^-} - e\Phi - \mu_{Cl^-}) \dot{C}_{Cl^-} \\ &+ \Big(\frac{\Theta_{\beta_H}}{C_b} + e\Phi + \Delta\mu_H - \mu_{H^+} \Big) C_b \dot{\beta}_H \\ &+ \Big(\frac{\Theta_{\beta_{Na}}}{C_b} + e\Phi + \Delta\mu_{Na} - \mu_{Na^+} \Big) C_b \dot{\beta}_{Na} \\ &+ (2\mu - \mu_{H^+} - \mu_{OH^-}) \Gamma_0 - \bar{u}_{dif} \le 0. \end{aligned} \tag{64}$$

Keeping in mind that $\mathbf{D}$, C, C_{H^+}, C_{Na^+}, C_{OH^-}, C_{Cl^-}, β_H, β_{Na}, Γ_0 are arbitrary functions and using Eq. (44), we conclude that

Eq. (64) is fulfilled, provided that the Cauchy stress tensor reads

$$\mathbf{T} = -\Pi\,\mathbf{I} + \frac{2}{J}(\mathbf{K}_{\rm mech} + \mathbf{K}_{\rm el}), \tag{65}$$

chemical potentials of water molecules and mobile ions are given by

$$\mu = \Theta_C + \Pi v, \qquad \mu_{\rm H^+} = \Theta_{\rm H^+} + e\Phi, \qquad \mu_{\rm Na^+} = \Theta_{\rm Na^+} + e\Phi,$$
$$\mu_{\rm OH^-} = \Theta_{\rm OH^-} - e\Phi, \qquad \mu_{\rm Cl^-} = \Theta_{\rm Cl^-} - e\Phi, \tag{66}$$

concentrations of non-ionized functional groups obey the equations

$$\frac{\Theta_{\beta_{\rm H}}}{C_{\rm b}} + e\Phi + \Delta\mu_{\rm H} - \mu_{\rm H^+} = 0,$$
$$\frac{\Theta_{\beta_{\rm Na}}}{C_{\rm b}} + e\Phi + \Delta\mu_{\rm Na} - \mu_{\rm Na^+} = 0, \tag{67}$$

volume expansion for the polymer network is governed by

$$\Big(\frac{2K}{3f} - W_{,f}\Big)\dot f = W_{,\alpha}\dot\alpha, \tag{68}$$

and the rate of association of $\rm H^+$, $\rm OH^-$ ions is determined by

$$\Gamma_0 = -\bar\Gamma(2\mu - \mu_{\rm H^+} - \mu_{\rm OH^-}), \tag{69}$$

where $\bar\Gamma$ is an arbitrary positive function.

H. Governing equations

Substitution of Eq. (A10) into Eqs. (66) implies that

$$\mu = \mu^0 + k_{\rm B}T\Big[\ln\frac{Cv}{1+Cv} + \frac{1}{1+Cv} + \frac{\chi}{(1+Cv)^2} + \frac{\Pi v}{k_{\rm B}T} - \frac{C_{\rm H^+} + C_{\rm Na^+} + C_{\rm OH^-} + C_{\rm Cl^-}}{C}\Big],$$

$$\mu_{\rm H^+} = \mu^0_{\rm H^+} + k_{\rm B}T\ln\frac{C_{\rm H^+}}{C} + e\Phi,$$
$$\mu_{\rm Na^+} = \mu^0_{\rm Na^+} + k_{\rm B}T\ln\frac{C_{\rm Na^+}}{C} + e\Phi, \tag{70}$$
$$\mu_{\rm OH^-} = \mu^0_{\rm OH^-} + k_{\rm B}T\ln\frac{C_{\rm OH^-}}{C} - e\Phi,$$
$$\mu_{\rm Cl^-} = \mu^0_{\rm Cl^-} + k_{\rm B}T\ln\frac{C_{\rm Cl^-}}{C} - e\Phi.$$

Insertion of Eqs. (70) and (A10) into Eq. (67) results in

$$\ln\frac{\beta_{\rm H}}{1-\beta_{\rm H}-\beta_{\rm Na}} - \ln\frac{C_{\rm H^+}}{C} + \ln {\rm K}'_{\rm H} = 0,$$
$$\ln\frac{\beta_{\rm Na}}{1-\beta_{\rm H}-\beta_{\rm Na}} - \ln\frac{C_{\rm Na^+}}{C} + \ln {\rm K}'_{\rm Na} = 0, \tag{71}$$

where

$${\rm K}'_{\rm H} = \exp\Big(\frac{\Delta\mu_{\rm H} - \mu^0_{\rm H^+}}{k_{\rm B}T}\Big), \qquad {\rm K}'_{\rm Na} = \exp\Big(\frac{\Delta\mu_{\rm Na} - \mu^0_{\rm Na^+}}{k_{\rm B}T}\Big). \tag{72}$$

When charged bound groups do not form ion pairs with $\rm Na^+$ ions, which implies that $\beta_{\rm Na} = 0$ and $\beta_{\rm H} = 1 - \alpha$, the first equality in Eq. (71) reads

$$\ln\frac{1-\alpha}{\alpha} - \ln\frac{C_{\rm H^+}}{C} + \ln {\rm K}'_{\rm H} = 0.$$

Resolving this equation with respect to α, we arrive at the conventional Henderson–Hasselbach equation

$$\alpha = {\rm K}'_{\rm H}\Big({\rm K}'_{\rm H} + \frac{C_{\rm H^+}}{C}\Big)^{-1}, \tag{73}$$

where $\rm K'_H$ coincides with the acid dissociation constant $\rm K'_a$,

$${\rm K}'_{\rm H} = {\rm K}'_{\rm a}. \tag{74}$$

In the general case, Eqs. (71) and (74) imply that

$$\beta_{\rm H} = \Big[1 + \frac{{\rm K}'_{\rm a}C}{C_{\rm H^+}}\Big(1 + \frac{C_{\rm Na^+}}{{\rm K}'_{\rm Na}C}\Big)\Big]^{-1},$$
$$\beta_{\rm Na} = \frac{{\rm K}'_{\rm a}C_{\rm Na^+}}{{\rm K}'_{\rm Na}C_{\rm H^+}}\Big[1 + \frac{{\rm K}'_{\rm a}C}{C_{\rm H^+}}\Big(1 + \frac{C_{\rm Na^+}}{{\rm K}'_{\rm Na}C}\Big)\Big]^{-1}. \tag{75}$$

Substitution of Eq. (75) into Eq. (10) yields

$$\alpha = {\rm K}'_{\rm a}\Big({\rm K}'_{\rm a} + \frac{C_{\rm H^+}}{C} + \frac{{\rm K}'_{\rm a}}{{\rm K}'_{\rm Na}}\frac{C_{\rm Na^+}}{C}\Big)^{-1}. \tag{76}$$

Equation (76) provides an extension of the Henderson–Hasselbach equation for PE gels where formation of ion pairs is taken into account between mobile cations $\rm Na^+$ and bound anions $\rm COO^-$.

It follows from Eqs. (69) and (70) that

$$\Gamma_0 = -\bar\Gamma k_{\rm B}T\Big[\Big(\frac{2\mu^0 - \mu^0_{\rm H^+} - \mu^0_{\rm OH^-}}{k_{\rm B}T} - \ln\frac{C_{\rm H^+}C_{\rm OH^-}}{C^2}\Big) + \Delta\mu\Big] \tag{77}$$

with

$$\Delta\mu = \ln\frac{Cv}{1+Cv} + \frac{1}{1+Cv} + \frac{\chi}{(1+Cv)^2} + \frac{\Pi v}{k_{\rm B}T} - \frac{C_{\rm H^+} + C_{\rm Na^+} + C_{\rm OH^-} + C_{\rm Cl^-}}{C}.$$

For a swollen gel ($Cv \gg 1$) in a bath with small concentrations of ions ($C_{\rm H^+}/C \ll 1$), $\Delta\mu$ is small compared with the term in parentheses. On the contrary, the coefficient $\bar\Gamma k_{\rm B}T$ is large compared with the characteristic rate of diffusion of solvent and solutes. To ensure that all terms in reaction-diffusion Eqs. (37) and (41) have the same order of smallness, one should require the expression in parentheses in Eq. (77) to vanish, which implies that (up to small terms)

$$\frac{C_{\rm H^+}C_{\rm OH^-}}{C^2} = \exp\Big(\frac{2\mu^0 - \mu^0_{\rm H^+} - \mu^0_{\rm OH^-}}{k_{\rm B}T}\Big).$$

Using notation (2) and (11), we find that this equality is equivalent to Eq. (3) with

$${\rm pK_w} = -\log\Big[\kappa^2\exp\Big(\frac{2\mu^0 - \mu^0_{\rm H^+} - \mu^0_{\rm OH^-}}{k_{\rm B}T}\Big)\Big]. \tag{78}$$

Formula (78) was derived in Ref. 41 by using another approach.

Combination of Eqs. (17), (A3), (A9), and (65) yields

$$\mathbf{T} = -\Pi\,\mathbf{I} + \frac{2}{1+Cv}\Big[W_{,1}\mathbf{B}_{\rm e} - J_{\rm e3}W_{,2}\mathbf{B}_{\rm e}^{-1} + (J_{\rm e2}W_{,2} + J_{\rm e3}W_{,3})\mathbf{I}\Big] + \mathbf{T}_{\rm M}, \tag{79}$$

where

$$\mathbf{T}_{\rm M} = \frac{1}{\epsilon}\Big[(\mathbf{h}\otimes\mathbf{h}) - \frac{1}{2}(\mathbf{h}\cdot\mathbf{h})\mathbf{I}\Big] \tag{80}$$

stands for the Maxwell stress.[42]

Although Eqs. (68), (79), and (80) describe development of stresses in a PE gel subjected to swelling, these relations (with W treated as a function of five arguments) appear to be overly complicated for practical applications. To simplify the model, we, first, disregard Maxwell stress (80) compared with the mechanical stress. Elementary estimates show that the characteristic Maxwell stress does not exceed 10^3 Pa, which is small compared with the characteristic elastic modulus of a gel whose order is 10^5 Pa. To further simplify the constitutive equations, a principle of electro-mechanical equivalence is introduced. According to this principle, an equivalent polymer network of non-charged chains exists with coefficient of volume expansion $f_{eq}(\alpha)$ and elastic energy $W_{eq}(J_{e1}, J_{e2}, J_{e3})$ depending on the principal invariants of the Cauchy–Green tensor for elastic deformation only such that the Cauchy stress in the real (partially ionized) network $\mathbf{T}$ coincides with the Cauchy stress in the non-ionized equivalent network

$$\mathbf{T} = -\Pi\,\mathbf{I} + \frac{2}{1+Cv}\Big[W_{eq,1}\mathbf{B}_e - J_{e3}W_{eq,2}\mathbf{B}_e^{-1} + (J_{e2}W_{eq,2} + J_{e3}W_{eq,3})\mathbf{I}\Big]. \tag{81}$$

This approach allows (i) differential Eq. (68) to be excluded from consideration by replacing it with a phenomenological equation for the function $f_{eq}(\alpha)$, and (ii) conventional formulas to be employed for the elastic energy W_{eq} instead of complicated expression (55). With reference to this concept, we omit the subscript "eq" in what follows, calculate the Cauchy stress tensor by means of Eq. (81), and postulate that the coefficient of volume expansion of the equivalent network f increases linearly with concentration of bound charges

$$f = 1 + q_0 + q_1 C_b \alpha, \tag{82}$$

where q_0 stands for degree of swelling of an as-prepared gel and q_1 is a material constant. Equation (82) is merely phenomenological, and the linear relation between f and α is chosen to reduce the number of adjustable parameters in the model. Another version of this equation, with f proportional to $\alpha^{\frac{2}{3}}$, is suggested by the anonymous reviewer based on the blob model for PE chains.[43]

Combination of Eqs. (41) and (42) results in the conventional reaction-diffusion equations for Na^+ and Cl^- ions

$$\begin{aligned}\dot{C}_{Na^+} &= \boldsymbol{\nabla}_0 \cdot \Big(\frac{D_{Na^+}C_{Na^+}}{k_B T}\mathbf{F}^{-1}\cdot\boldsymbol{\nabla}_0\mu_{Na^+}\cdot\mathbf{F}^{-1}\Big) - \dot{\beta}_{Na}C_b,\\ \dot{C}_{Cl^-} &= \boldsymbol{\nabla}_0 \cdot \Big(\frac{D_{Cl^-}C_{Cl^-}}{k_B T}\mathbf{F}^{-1}\cdot\boldsymbol{\nabla}_0\mu_{Cl^-}\cdot\mathbf{F}^{-1}\Big).\end{aligned} \tag{83}$$

Diffusion of water molecules and H^+, OH^- ions is governed by Eqs. (37), (41), and (42)

$$\begin{aligned}\dot{C} &= \boldsymbol{\nabla}_0 \cdot \Big(\frac{DC}{k_B T}\mathbf{F}^{-1}\cdot\boldsymbol{\nabla}_0\mu\cdot\mathbf{F}^{-1}\Big) + 2\Gamma_0,\\ \dot{C}_{H^+} &= \boldsymbol{\nabla}_0 \cdot \Big(\frac{D_{H^+}C_{H^+}}{k_B T}\mathbf{F}^{-1}\cdot\boldsymbol{\nabla}_0\mu_{H^+}\cdot\mathbf{F}^{-1}\Big) - \Gamma_0 - \dot{\beta}_H C_b,\\ \dot{C}_{OH^-} &= \boldsymbol{\nabla}_0 \cdot \Big(\frac{D_{OH^-}C_{OH^-}}{k_B T}\mathbf{F}^{-1}\cdot\boldsymbol{\nabla}_0\mu_{OH^-}\cdot\mathbf{F}^{-1}\Big) - \Gamma_0.\end{aligned}$$

To exclude Γ_0, we sum all relations and subtract the third equation from the second one,

$$\begin{aligned}&\frac{\partial}{\partial t}(C + C_{H^+} + C_{OH^-})\\ &\quad= \boldsymbol{\nabla}_0 \cdot \Big[\frac{1}{k_B T}\mathbf{F}^{-1}\cdot\Big(DC\boldsymbol{\nabla}_0\mu + D_{H^+}C_{H^+}\boldsymbol{\nabla}_0\mu_{H^+}\\ &\qquad + D_{OH^-}C_{OH^-}\boldsymbol{\nabla}_0\mu_{OH^-}\Big)\cdot\mathbf{F}^{-1}\Big] - \dot{\beta}_H C_b,\\ &\frac{\partial}{\partial t}(C_{H^+} - C_{OH^-})\\ &\quad= \boldsymbol{\nabla}_0 \cdot \Big[\frac{1}{k_B T}\mathbf{F}^{-1}\cdot\Big(D_{H^+}C_{H^+}\boldsymbol{\nabla}_0\mu_{H^+}\\ &\qquad - D_{OH^-}C_{OH^-}\boldsymbol{\nabla}_0\mu_{OH^-}\Big)\cdot\mathbf{F}^{-1}\Big] - \dot{\beta}_H C_b.\end{aligned} \tag{84}$$

Presuming the rate of self-ionization of water to exceed strongly the rate of diffusion, we conclude from Eq. (69) that these equations are accompanied by the nonlinear equation

$$2\mu - \mu_{H^+} - \mu_{OH^-} = 0. \tag{85}$$

Similar relations for the one-dimensional case were recently derived in Ref. 44.

Constitutive equations for a PE gel involve (i) stress–strain relation (81), (ii) Eq. (70) for chemical potentials of solvent and solutes, (iii) Eqs. (75) and (76) for degree of ionization of chains, and (iv) Eq. (82) for the coefficient of inflation of the equivalent network induced by dissociation of functional groups. These relations are accompanied by (i) the equilibrium equation for the Cauchy stress tensor, (ii) Poisson's Eq. (30) for electrostatic potential, and (iii) algebraic–differential Eqs. (83)–(85) for transport of solvent and solute.

III. EQUILIBRIUM SWELLING

To examine the ability of the model to describe observations on PE gels, we simplify the governing equations for equilibrium swelling accompanied by a homogeneous deformation and apply them to fit experimental data. With reference to Ref. 45, it is assumed that in a gel specimen fully swollen under homogeneous deformation,

1. concentrations of solvent and solutes are independent of spatial coordinates;
2. electrostatic potential is independent of spatial coordinates but adopts different values, Φ and $\bar{\Phi}$, in the gel and in the bath. The difference between these quantities characterizes strength of an electric double layer on the boundary of a sample (whose thickness is disregarded compared with the characteristic size of the specimen).

To approximate observations, the neo–Hookean formula is adopted for the strain energy density

$$W = \frac{1}{2}G\Big[(J_{e1} - 3) - \ln J_{e3}\Big], \tag{86}$$

where G stands for shear modulus. The physical meaning of Eq. (86) with J_{e1}, J_{e3} as arguments of the function W was discussed in Ref. 46 where this formula was "re-derived" within the concept of entropic elasticity by using an approach proposed in Ref. 47. More sophisticated expressions for this function were developed in Refs. 48 and 49. Inserting Eq. (86)

into Eq. (81), we arrive at the stress–strain relation

$$\mathbf{T} = -\Pi\,\mathbf{I} + \frac{G}{1+Cv}(\mathbf{B}_e - \mathbf{I}). \tag{87}$$

A. Donnan equilibrium

Under equilibrium conditions, chemical potentials of solvent and solutes in a gel specimen and in the bath coincide

$$\mu = \bar{\mu}, \qquad \mu_{H^+} = \bar{\mu}_{H^+}, \qquad \mu_{Na^+} = \bar{\mu}_{Na^+}, \qquad \mu_{OH^-} = \bar{\mu}_{OH^-}, \qquad \mu_{Cl^-} = \bar{\mu}_{Cl^-}, \tag{88}$$

where the bar denotes parameters of the bath. Substituting Eq. (70) into Eq. (88) and using Eq. (76), we arrive at the equations (Appendix B)

$$X\Big(X - \alpha\frac{Q_b}{Q}\Big) = \frac{1}{\kappa^2}(10^{-pH} + \theta)^2, \tag{89}$$

$$\alpha = K'_a\Big[K'_a + \frac{X}{10^{-pH}+\theta}\Big(10^{-pH} + R\theta\Big)\Big]^{-1}, \tag{90}$$

$$\ln\frac{Q}{1+Q} + \frac{1}{1+Q} + \frac{\chi}{(1+Q)^2} + \frac{\Pi v}{k_B T} - X\Big(\alpha\frac{Q_b}{Q}\Big)^2\Big(X + \frac{1}{\kappa}(10^{-pH}+\theta)\Big)^{-2} = 0, \tag{91}$$

where

$$Q = Cv, \qquad Q_b = C_b v, \qquad X = \frac{C_{H^+} + C_{Na^+}}{C}, \qquad R = \frac{K'_a}{K'_{Na}}. \tag{92}$$

B. Unconstrained swelling

Under unconstrained swelling of a gel specimen, the deformation gradient for macro-deformation reads

$$\mathbf{F} = (1+Cv)^{\frac{1}{3}}\mathbf{I}. \tag{93}$$

Substitution of Eqs. (82) and (93) into Eq. (47) yields

$$\mathbf{F}_e = \Big(\frac{1+Cv}{1+q_0+q_1C_b\alpha}\Big)^{\frac{1}{3}}\mathbf{I}. \tag{94}$$

It follows from Eqs. (51), (87), and (94) that

$$\mathbf{T} = T\mathbf{I}, \qquad T = -\Pi + \frac{G}{1+Cv}\Big[\Big(\frac{1+Cv}{1+q_0+q_1C_b\alpha}\Big)^{\frac{2}{3}} - 1\Big].$$

Keeping in mind that $\mathbf{T} = \mathbf{0}$ for a specimen with a traction-free surface, we find that

$$\Pi = \frac{G}{1+Cv}\Big[\Big(\frac{1+Cv}{1+q_0+q_1C_b\alpha}\Big)^{\frac{2}{3}} - 1\Big].$$

Inserting this expression into Eq. (91), using Eq. (92), and setting

$$g = \frac{Gv}{k_B T}, \qquad \bar{q} = \frac{q_1}{v}Q_b, \tag{95}$$

we find that

$$\ln\frac{Q}{1+Q} + \frac{1}{1+Q} + \frac{\chi}{(1+Q)^2} + \frac{g}{1+Q}\Big[\Big(\frac{1+Q}{1+q_0+\bar{q}\alpha}\Big)^{\frac{2}{3}} - 1\Big] - X\Big(\alpha\frac{Q_b}{Q}\Big)^2\Big(X + \frac{1}{\kappa}(10^{-pH}+\theta)\Big)^{-2} = 0. \tag{96}$$

C. Constrained swelling

A dry gel in the form of a disk is immersed into a rigid cell whose internal cross-section coincides with that of the sample. We introduce a Cartesian frame $\{X_m\}$ $(m = 1,2,3)$ in the initial state with unit vectors $\mathbf{e}_m$. Swelling of the sample occurs when the cell is dipped into water. As walls of the cell prevent extension in the transverse directions (determined by vectors $\mathbf{e}_2$ and $\mathbf{e}_3$), deformation of the disk occurs in the direction $\mathbf{e}_1$ only. According to Eq. (17), the deformation gradient for macro-deformation reads

$$\mathbf{F} = (1+Cv)\mathbf{e}_1\otimes\mathbf{e}_1 + \mathbf{e}_2\otimes\mathbf{e}_2 + \mathbf{e}_3\otimes\mathbf{e}_3. \tag{97}$$

Equation (97) describes constrained swelling of cylindrical specimens[50] and swelling of thin hydrogel films grown on rigid substrates.[51]

It follows from Eqs. (47), (82), and (97) that

$$\mathbf{F}_e = \frac{1}{(1+q_0+q_1C_b\alpha)^{\frac{1}{3}}}\times\Big[(1+Cv)\mathbf{e}_1\otimes\mathbf{e}_1 + (\mathbf{e}_2\otimes\mathbf{e}_2 + \mathbf{e}_3\otimes\mathbf{e}_3)\Big]. \tag{98}$$

Insertion of Eq. (98) into Eq. (87) implies that

$$\mathbf{T} = T_1\mathbf{e}_1\otimes\mathbf{e}_1 + T_2(\mathbf{e}_2\otimes\mathbf{e}_2 + \mathbf{e}_3\otimes\mathbf{e}_3)$$

with

$$T_1 = -\Pi + \frac{G}{1+Cv}\Big[\frac{(1+Cv)^2}{(1+q_0+q_1C_b\alpha)^{\frac{2}{3}}} - 1\Big],$$

$$T_2 = -\Pi + \frac{G}{1+Cv}\Big[\frac{1}{(1+q_0+q_1C_b\alpha)^{\frac{2}{3}}} - 1\Big].$$

The equilibrium equation and the traction-free boundary conditions at the faces of the disk imply that $T_1 = 0$. Combination of these equations results in

$$\Pi = \frac{G}{1+Cv}\Big[\frac{(1+Cv)^2}{(1+q_0+q_1C_b\alpha)^{\frac{2}{3}}} - 1\Big]. \tag{99}$$

Inserting Eq. (99) into Eq. (91) and using Eqs. (92) and (95), we arrive at the formula

$$\ln\frac{Q}{1+Q} + \frac{1}{1+Q} + \frac{\chi}{(1+Q)^2} + \frac{g}{1+Q}\Big[\frac{(1+Q)^2}{(1+q_0+\bar{q}\alpha)^{\frac{2}{3}}} - 1\Big] - X\Big(\alpha\frac{Q_b}{Q}\Big)^2\Big(X + \frac{1}{\kappa}(10^{-pH}+\theta)\Big)^{-2} = 0. \tag{100}$$

For each pH and molar fraction of salt in the bath θ, Eqs. (89), (90), (96), and (100) determine degree of swelling Q, degree of ionization of chains α, and concentration of positively charged mobile ions X. These relations involve seven

material constants: (i) g stands for the dimensionless elastic modulus, (ii) Q_b is volume occupied by functional groups in the initial state, (iii) K_a' denotes the dissociation constant for these groups, (iv) R is the ratio of dissociation constants for carboxyl groups and ion pairs, (v) χ is the Flory–Huggins parameter, and (vi) q_0, $\bar{q}$ describe evolution of the stress-free state of polymer chains induced by their ionization.

Although Eqs. (89), (90), (96), and (100) appear to be novel, it is worth mentioning similarities between them and governing equations for equilibrium swelling developed in previous studies. Equation (89) resembles conventional relations for the Donnan equilibrium. Analogs of Eq. (90) were derived in Refs. 19 and 20. Expressions for ionic pressure similar to the last terms in Eqs. (96) and (100) were proposed in Ref. 52. The novelty of our approach consists in the presence of a term proportional to α in the expression for osmotic pressure Π.

IV. FITTING OF OBSERVATIONS

To demonstrate the ability of Eqs. (89), (90), (96), and (100) to describe equilibrium swelling diagrams, these relations are solved by the Newton–Raphson algorithm, and results of simulation are compared with experimental data. To reduce the number of material constants used in the numerical analysis, we set $q_0 = 0$ (the reference state of a gel with non-ionized functional groups coincides with the initial state) and $\chi = 0.4$ (water is treated as a poor solvent).

A. Poly(acrylic acid) gel

We begin with the analysis of experimental data on poly(acrylic acid) gel under unconstrained swelling reported in Figures 1 and 2. The gel was prepared by free radical polymerization of acrylic acid (AAc) monomers in an aqueous solution (700 mM) at room temperature by using N,N'-methylenebis(acrylamide) (BAAm) (7 mM) as a cross-linker, ammonium peroxodisulfate (APS) (3.5 mM) as an initiator, N,N,N',N'-tetramethylethylenediamine (TEMED) (8 μM) as an accelerator.[53] In Figure 1, equilibrium degree of swelling

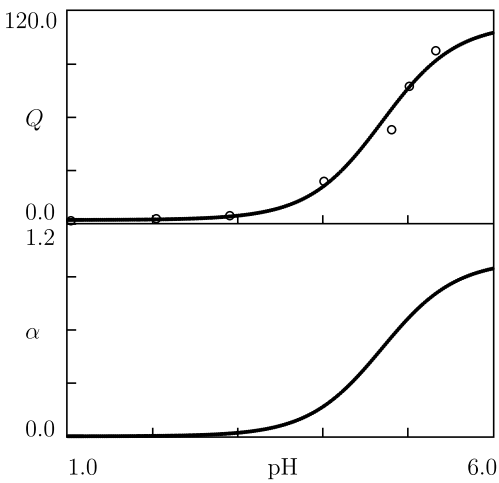

FIG. 1. Degree of swelling Q and degree of ionization α versus pH. Circles: experimental data on AAc gel.[53] Solid lines: results of simulation.

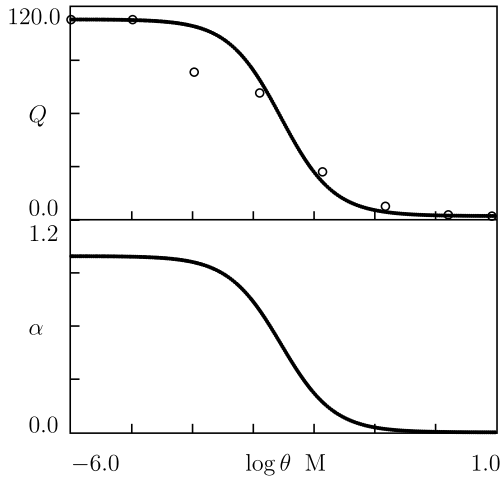

FIG. 2. Degree of swelling Q and degree of ionization α versus molar fraction θ of salt. Circles: experimental data on AAc gel.[53] Solid lines: results of simulation.

Q is plotted versus pH for $\theta = 0$. In Figure 2, Q is depicted versus molar fraction θ of salt ($NaNO_3$) at pH = 7.

To approximate observations in Figure 1, we set $Q_b = 5.0 \times 10^{-7}$, determine elastic modulus $g = 7.0 \times 10^{-2}$ by matching the data at low pH, and find $pK_a = 4.7$ (with $K_a = \kappa K_a'$) and $\bar{q} = 111.5$ from the best-fit condition for the entire swelling curve. It is worth noting that pK_a calculated by matching the experimental data coincides with that determined experimentally in Ref. 20 and found by means of the Debuy–Huckel theory in Ref. 54, and it exceeds only slightly dissociation constant $pK_a = 4.35$ for a dilute solution of AAc chains.

Fitting of observations in Figure 2 is performed with the material constants found by matching the experimental data in Figure 1. The only adjustable parameter $R = 7.0 \times 10^{-3}$ is determined from the best-fit condition for the entire swelling diagram.

To examine the effects of pH and molar fraction of salt on degree of ionization α, results of numerical analysis are reported in Figures 1 and 2. Figure 1 demonstrates that α vanishes at low pH, increases monotonically with pH, and reaches its ultimate value $\alpha = 1$ at pH = 6. According to Figure 2, $\alpha = 1$ at low concentrations of salt ($\theta < 10^{-4}$M), decreases monotonically with θ, and vanishes at $\theta > 0.1$M.

To evaluate combined effects of pH and ionic strength on the equilibrium water uptake under unconstrained swelling, Eqs. (89), (90), and (96) are solved numerically with the material constants found by matching observations in Figures 1 and 2. Results of simulation are presented in Figure 3 where Q and α are depicted versus θ for various pH. The following conclusions are drawn: (i) at pH = 2, degree of swelling Q is independent of molar fraction of salt θ because functional groups remain uncharged, (ii) at pH in the interval between 3 and 6, Q strongly increases with pH (by two orders of magnitude) at $\theta < 1$ mM, (iii) with the growth of molar fraction of salt, the effect of pH weakens, and it disappears when θ reaches 0.1M, (iv) at high pH (exceeding 6), its influence on the equilibrium swelling diagrams becomes of secondary importance, (v) for each pH under investigation,

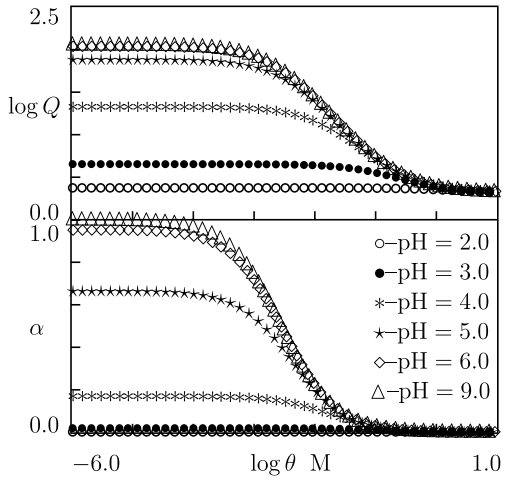

FIG. 3. Degree of swelling Q and degree of ionization α versus molar fraction θ of salt. Symbols: results of simulation for unconstrained swelling of AAc gel at various pH.

degree of ionization α reaches its maximum value α_{max} at low ionic strengths of solution, decreases monotonically with θ, and vanishes when θ exceeds 0.1M, (vi) the maximum degree of ionization α_{max} increases monotonically with pH and approaches its ultimate value $\alpha_{max} = 1$ at pH > 6.

To assess how the degree of swelling Q and degree of ionization α are affected by macro-deformation, numerical analysis of Eqs. (89), (90), and (100) is performed with the same material constants. Results of simulation for constrained swelling of AAc gel are reported in Figure 4. Comparison of Figures 3 and 4 leads to the following conclusions: (i) equilibrium degree of swelling Q decays strongly (by two orders of magnitude) when constraints are imposed on deformation, (ii) under constraints, the influence of pH on water uptake becomes less pronounced (Q increases with pH by a factor of 5 for constrained swelling compared with its growth by a factor of 120 for unconstrained swelling), (iii) evolution of water uptake with ionic strength becomes non-monotonic under constrained swelling: at pH > 4, Q increases with θ at $\theta < 0.1$ mM, reaches its maximum, and decreases strongly afterwards, (iv) the growth of Q with θ at small molar fractions of salt is accompanied by non-monotonic changes in degree of ionization α which reaches its maximum value at $\theta = 0.1$ mM.

Observations on non-monotonic changes in degree of swelling of a thin film with concentration of salt were reported in Refs. 55 and 56, where a model was suggested to describe the experimental data. This phenomenon was earlier predicted within the self-consistent field theory of PE brushes in Ref. 57. Very recently, it was investigated by molecular dynamics simulation for PE chains grafted on a solid surface.[58] An advantage of our model is that it predicts qualitatively this effect without introduction of additional hypotheses and demonstrates that the non-monotonicity is intimately connected with constraints imposed on macro-deformation of a PE gel.

We proceed with the analysis of observations of AAc gel prepared by radical polymerization of AAc monomers in aqueous solution (2.78M) by using BAAm (1 mM) as a cross-linker and potassium persulfate (KPS) (1 mM) as an initiator.[59] Swelling tests were performed in McIlvaine phosphate-citrate buffer solution with $\theta = 0.5$M at room temperature. Experimental data are depicted in Figure 5 where equilibrium degree of swelling Q is plotted versus pH. To fit these observations, we fix $pK_a = 4.7$ (according to Eqs. (72) and (74), this parameter is independent of molar fraction of salt), set $Q_b = 1.39 \times 10^{-6}$ (volume fraction of functional groups in the dry state is proportional to concentration of monomers in a pre-gel solution), calculate $g = 0.03$ by matching data at low pH, and find $\bar{q} = 29.0$, $R = 2.5 \times 10^{-5}$ from the best-fit condition for the entire swelling curve. A decrease in $\bar{q}$ compared with the data depicted in Figures 1 and 2 is explained by an increase in the number of monomers between cross-links. According to Eq. (72) and (92), a decay in R implies that $\delta\mu_{buffer}$ is higher than $\delta\mu_{Na}$, where $\delta\mu$ stands for the difference between $\Delta\mu$ and μ^0 in Eq. (72) for the corresponding species (calculations show that strength $\delta\mu$ of ion pairs formed by charged carboxyl groups with cations

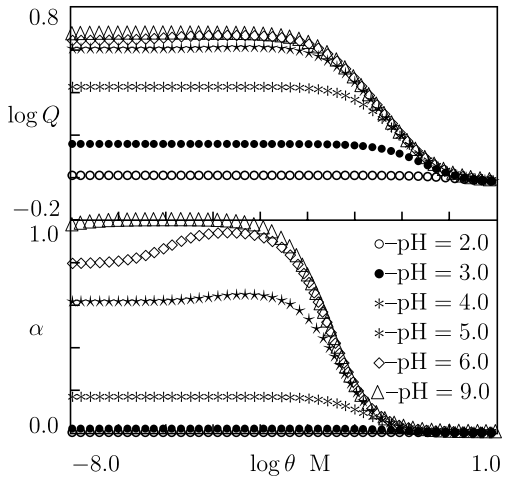

FIG. 4. Degree of swelling Q and degree of ionization α versus molar fraction θ of salt. Symbols: results of simulation for constrained swelling of AAc gel at various pH.

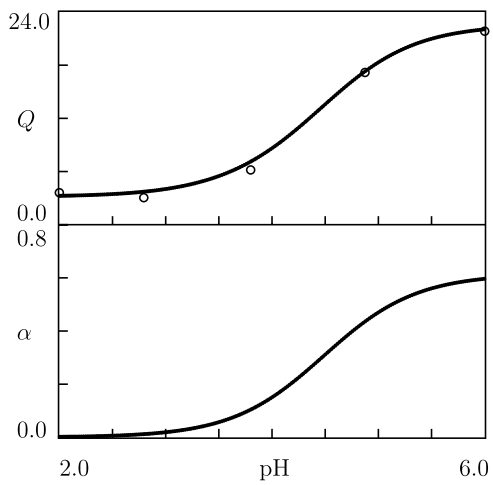

FIG. 5. Degree of swelling Q and degree of ionization α versus pH. Circles: experimental data on AAc gel in buffer solution with $\theta = 0.5$ M.[59] Solid lines: results of simulation.

from the buffer exceeds that for Na^+COO^- ion pairs by $5.63k_BT$).

B. DMAA-AMPS gels

To examine how concentration of functional groups affects equilibrium water uptake, we analyze swelling diagrams on poly(*N*,*N*-dimethylacrylamide-co-(2-(acrylamido)-2-methylpropane-sulfonic acid)) (DMAA–AMPS) copolymer gels.[60] Samples were prepared by polymerization of monomers in an aqueous solution (0.75M) by using BAAm (17 mM) as a cross-linker. Molar fraction of anionic AMPS monomers φ in the pre-gel solution varied from 0.1 to 0.7. Swelling tests were conducted at room temperature in aqueous solutions of NaCl with pH = 7. Experimental data are presented in Figure 6 where Q is plotted versus θ.

We start with approximation of the swelling curve for gel with $\varphi_{max} = 0.7$, fix $pK_a = 4.0$ (in accord with Refs. 61 and 62), set $Q_{b\,max} = 2.0 \times 10^{-6}$, find $g = 2.0 \times 10^{-3}$ by matching observations at $\theta = 1$M, and determine $\bar{q}$ and $R = 0.13$ from the best-fit condition for the entire diagram. Matching experimental data for the other gels is conducted with fixed pK_a and R values. Parameter Q_b is determined from the equation

$$Q_b = \frac{\varphi}{\varphi_{max}} Q_{b\,max}, \tag{101}$$

which means that concentration of functional groups is proportional to molar fraction of AMPS monomers. Each swelling diagram is fitted separately by means of two parameters, g and $\bar{q}$. The effect of φ on these quantities is illustrated in Figure 7 where the data are approximated by the equations

$$g = g_0 + g_1\varphi, \qquad \log \bar{q} = \bar{q}_0 + \bar{q}_1\varphi \tag{102}$$

with coefficients calculated by the least-squares technique.

To reveal the ability of the model to predict observations, simulation of Eqs. (89), (90), and (96) is conducted for unconstrained swelling of copolymer gels in aqueous solutions with a fixed concentration of salt $\theta = 1$ mM and various pH.

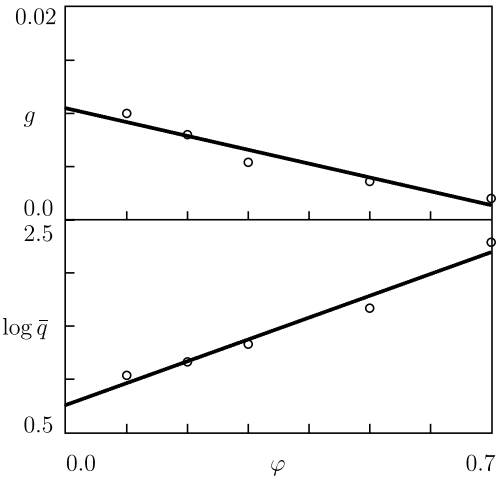

FIG. 7. Coefficients g and $\bar{q}$ versus molar fraction φ of AMPS monomers. Circles: treatment of observations. Solid lines: approximation of the data by Eq. (102).

Results of numerical analysis are depicted in Figure 8. This figure shows that Q increases with φ for a given pH and grows monotonically with pH for a fixed φ. A noticeable increase in Q with pH starts near pH = 2, and Q reaches its ultimate value in the vicinity of pH = 5. All conclusions are in quantitative agreement with observations on cross-linked cellulose-AMPS copolymer gels.[63]

To evaluate the effect of ionic strength of solution on degree of swelling and degree of ionization of DMAA–AMPS gel, Eqs. (89), (90), and (96) are solved numerically with the material constants found for $\varphi = 0.7$. Results of simulation with $\theta = 0.01$, 1.0, and 10.0 mM are reported in Figure 9 where Q and α are plotted versus pH. The following conclusions are drawn: (i) given θ, parameters Q and α increase monotonically with pH and approach their ultimate values, (ii) these values decrease strongly with concentration of salt θ, and (iii) the pH values, at which Q and α reach their maxima, are reduced with θ. These conclusions are in accord with observations on copolymer gels reported in Ref. 54.

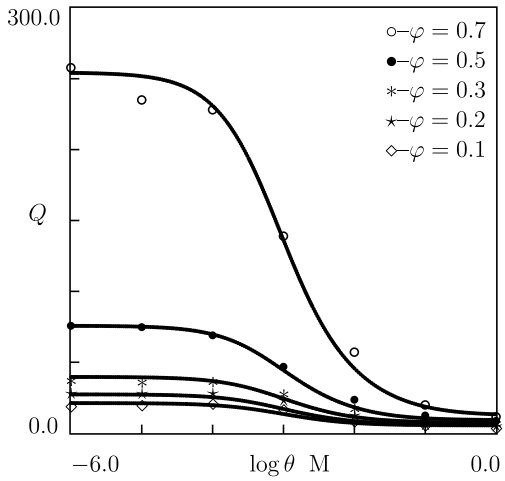

FIG. 6. Degree of swelling Q versus molar fraction of salt θ. Symbols: experimental data on DMAA-AMPS gels with various molar fractions φ of AMPS monomers.[60] Solid lines: results of simulation.

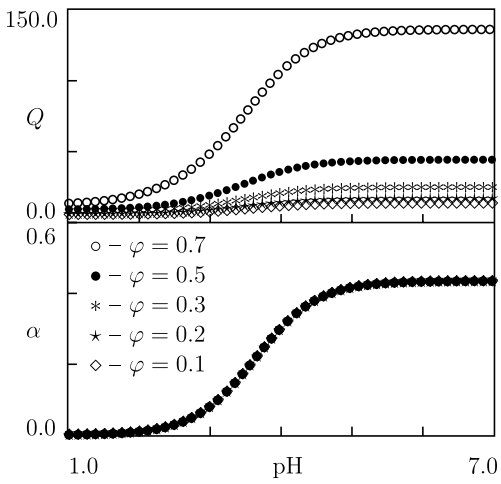

FIG. 8. Degree of swelling Q and degree of ionization α versus pH of buffer solution with $\theta = 1$ mM. Symbols: results of simulation for unconstrained swelling of AMPS-DMAA gels with various molar fractions φ of AMPS monomers.

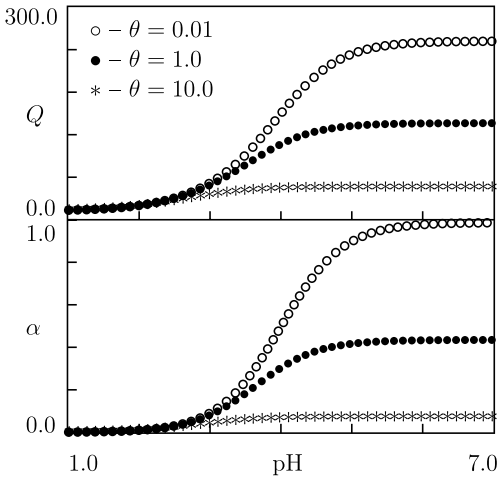

FIG. 9. Degree of swelling Q and degree of ionization α versus pH of buffer solutions with various molar fractions θ mM. Symbols: results of simulation for unconstrained swelling of AMPS-DMAA gel with $\varphi = 0.7$.

To assess the effect of constraints on swelling and ionization of PE gels, simulation of Eqs. (89), (90), (96), and (100) is performed for DMAA–AMPS gel with $\varphi = 0.7$ immersed into an aqueous solution of salt with $\theta = 0.1$ mM. Results of numerical analysis are depicted in Figure 10. This figure demonstrates that degree of swelling Q decreases strongly, while degree of ionization α remains practically unaffected by the presence of constraints.

C. Copolymer gels in the entire interval of pH values

Figures 8–10 demonstrate that equilibrium degree of swelling Q increases with pH and approaches its maximum at pH values in the vicinity of pH = 7. Observations show that under further growth of pH (to ensure it, sodium hydroxide NaOH is conventionally immersed into the bath instead of hydrochloric acid), Q remains constant until it starts to decay at pH ≥ 9.

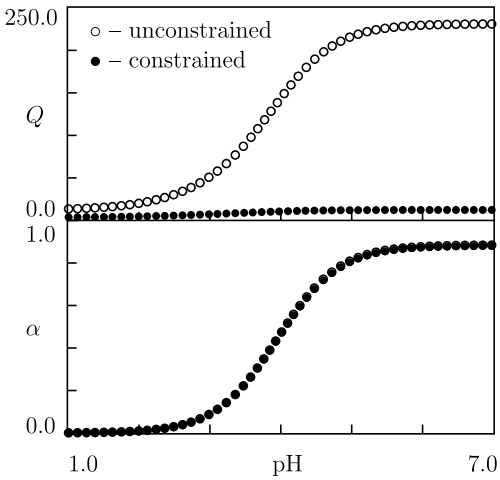

FIG. 10. Degree of swelling Q and degree of ionization α versus pH of buffer solution with $\theta = 0.1$ mM. Symbols: results of simulation for unconstrained and constrained swelling of AMPS-DMAA gel with $\varphi = 0.7$.

Although the constitutive model has been derived for the case pH ≤ 7 (when pH is altered by addition of HCl to the bath, see Eq. (4)), it can be shown that Eqs. (89), (90), (96), and (100) remain valid for arbitrary pH values, provided that θ (molar fraction of mobile cations that differ from hydroxide ions) is determined with account for dissociation of NaOH

$$\mathrm{NaOH} \rightleftarrows \mathrm{Na^+} + \mathrm{OH^-}.$$

When no salt is dissolved in a water bath, parameter θ reads

$$\theta = 0 \quad (\mathrm{pH} \le 7), \qquad \theta = 10^{\mathrm{pH}-\mathrm{pK_w}} - 10^{-\mathrm{pH}} \quad (\mathrm{pH} > 7). \tag{103}$$

The first equality in Eq. (103) means that the bath contains no Na^+ ions when HCl is added to change its pH. The other equality follows from Eqs. (2) and (3) together with the electro-neutrality condition $[Na^+] + [H^+] = [OH^-]$ for the bath with entirely dissociated sodium hydroxide.

To demonstrate that the model with θ given by Eq. (103) describes equilibrium swelling diagrams in the entire interval of pH values, observations are fitted on poly(*N*-isopropylacrylamide-co-methacrylic acid) (NIPA–MAc) copolymer gels.[64] Microgel particles were prepared by dispersion polymerization of monomers in aqueous solution (6 g/l) at 70 °C by using BAAm (1 mol. %) as a cross-linker and APS (0.26 g/l) as an initiator. Experimental data on gels with molar fractions of MAc $\varphi = 0.024$, 0.082, and 0.23 under unconstrained swelling at room temperature are depicted in Figure 11 where the dimensionless volume of a microgel particle $\bar{V} = V/V_0$ is plotted versus pH (V_0 stands for the volume of a particle with uncharged functional groups).

We begin with fitting observations for the gel with $\varphi_{\max} = 0.23$, fix $\mathrm{pK_a} = 5.0$ in accord with Ref. 65, and set $Q_{\mathrm{b\,max}} = 2.0 \times 10^{-7}$, $g = 1.5 \times 10^{-3}$. Parameters R and $\bar{q}$ are found from the best-fit condition for the entire swelling curve with $\bar{V}$ given by

$$\bar{V} = \frac{1+Q}{1+Q|_{\mathrm{pH}=0}}.$$

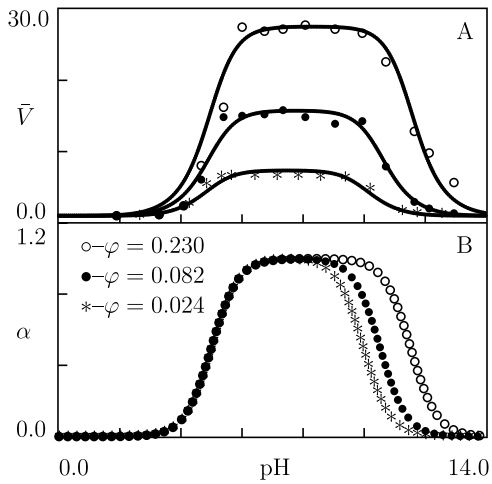

FIG. 11. (a) Dimensionless volume of a microgel particle $\bar{V}$ versus pH. Symbols: experimental data on NIPA-MAc gels with various molar fractions φ of MAc under unconstrained swelling.[64] Solid lines: results of simulation. (b) Degree of ionization α versus pH. Symbols: results of simulation.

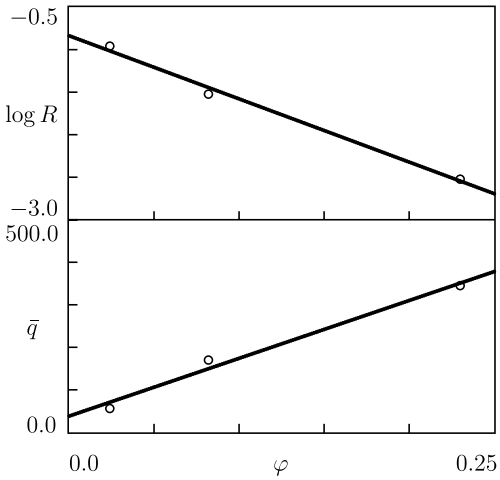

FIG. 12. Coefficients R and $\bar{q}$ versus molar fraction φ of MAc. Circles: treatment of observations. Solid lines: approximation of the data by Eq. (104).

Matching experimental data on microgels with other φ is conducted with the help of two adjustable parameters, R and $\bar{q}$, under the assumptions that Q_b is given by Eq. (101) and pK_a, g are independent of φ.

Evolution of parameters R and $\bar{q}$ with molar fraction φ of MAc is illustrated in Figure 12. The data are approximated by the equations

$$\log R = R_0 + R_1\varphi, \qquad \bar{q} = \bar{q}_0 + \bar{q}_1\varphi, \tag{104}$$

where the coefficients are calculated by the least-squares method. Figure 12 shows that (i) $\bar{q}$ increases noticeably with φ, in qualitative agreement with the data depicted in Figure 7, and (ii) R decreases strongly with φ (this decay is responsive for the reduction of $\bar{V}$ at high pH).

To assess how equilibrium water uptake is affected by constraints, simulation is performed of Eqs. (89), (90), (100), and (103) with the material parameters determined by fitting observations in Figure 11. Results of numerical analysis are reported in Figure 13 where degree of swelling Q and degree of ionization α are plotted versus pH. The following conclusions are drawn from Figures 11 and 13: (i) under constrained swelling, a decay in Q with pH in the region pH > 7 starts at smaller pH values than under unconstrained water uptake, (ii) the rate of decrease in Q with pH under unconstrained swelling exceeds strongly that under constrained swelling, (iii) changes in degree of ionization of chains α with pH are practically independent of constraints.

To reveal the ability of the model to predict experimental data, observations are studied on poly(acrylamide-co-sodium acrylate) gel prepared by free-radical copolymerization of acrylamide (632 mM) and sodium acrylate (71.2 mM) monomers in an aqueous solution at room temperature by using BAAm (8.6 mM) as a cross-linker, APS (1.75 mM) as an initiator, and sodium metabisulfite (2.1 mM) as an accelerator.[66]

We begin with the analysis of equilibrium swelling diagram depicted in Figure 14, where Q is plotted versus pH of a bath without salt. In the fitting procedure, we set $Q_b = 2.0 \times 10^{-8}$, determine $g = 0.14$ by matching data at low pH, and find $pK_a = 6.3$, $\bar{q} = 29.6$, $R = 2.6 \times 10^{-4}$ from the best-fit condition for the entire curve. To assess changes in degree of ionization of chains with pH, results of simulation for the function α(pH) are also presented in Figure 14.

We proceed with the analysis of equilibrium water uptake by the same gel immersed into a water bath with pH = 7 and various molar fractions θ of dissolved $NaNO_3$ salt. Figure 15 presents experimental data reported in Ref. 66 together with results of numerical analysis with the material constants determined by fitting observations in Figure 14. Good agreement is demonstrated in Figure 15 between the observations and their predictions by the model.

D. Discussion

Two types of non-monotonicity are revealed in simulation: (i) the non-monotonic dependence of the equilibrium degree of swelling Q on concentration of salt θ under constrained swelling (Figure 4) and (ii) the non-monotonic

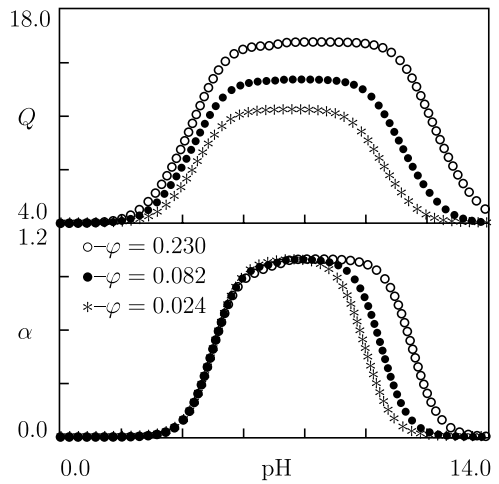

FIG. 13. Degree of swelling Q and degree of ionization α versus pH. Symbols: results of simulation for constrained swelling of NIPA-MAc gels with various molar fractions φ of MAc.

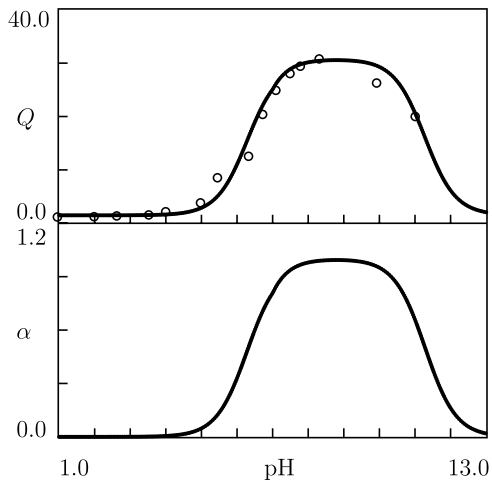

FIG. 14. Degree of swelling Q and degree of ionization α versus pH. Circles: experimental data on poly(acrylamide-co-sodium acrylate) gel under unconstrained swelling.[66] Solid lines: results of simulation.

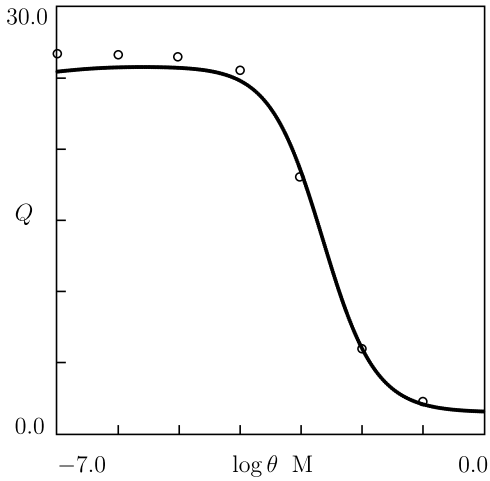

FIG. 15. Degree of swelling Q versus molar fraction θ of salt. Circles: experimental data on poly(acrylamide-co-sodium acrylate) gel under unconstrained swelling.[66] Solid line: prediction of the model.

dependence of Q on pH under unconstrained swelling (Figures 11 and 14).

The former phenomenon is observed when constraints are imposed on water uptake and degree of swelling Q remains relatively small (compared with Q under unconstrained swelling). To demonstrate that this condition is important, we focus on the analysis of the last term in Eqs. (96) and (100) that denotes the dimensionless ionic pressure

$$\Pi_{\rm ion} = X\Big(\alpha\frac{Q_{\rm b}}{Q}\Big)^2\Big(X+\frac{1}{\kappa}(10^{-\rm pH}+\theta)\Big)^{-2}.$$

Expressing the term $a = \alpha Q_{\rm b}/Q$ from Eq. (B15) and inserting it into this relation, we find that

$$\Pi_{\rm ion} = \frac{(X-\xi)^2}{X} \tag{105}$$

with $\xi = (10^{-\rm pH}+\theta)/\kappa$. In the new notation, Eq. (89) reads

$$X^2 - aX - \xi^2 = 0. \tag{106}$$

At relatively small degrees of swelling Q, it is natural to presume a to be large, and the ratio ξ/a to be small compared with unity. Under the condition $\eta = \xi/a \ll 1$, the leading term in the solution of Eq. (106) is given by

$$X = a + \frac{\xi^2}{a}. \tag{107}$$

Substitution of Eq. (107) into Eq. (105) implies that

$$\Pi_{\rm ion} = \frac{(1-\eta+\eta^2)^2}{1+\eta^2}.$$

It follows from this equation that $\Pi_{\rm ion}$ is a non-monotonic function of η which decreases at $\eta < \eta_{\rm min} = 0.682$ and increases at $\eta > \eta_{\rm min}$. Keeping in mind that η is proportional to concentration of salt θ, we conclude that the non-monotonic dependence of Q on θ under constrained swelling reflects the non-monotonic dependence of ionic pressure on this parameter. Under unconstrained swelling with large Q, the above arguments do not work, $\Pi_{\rm ion}$ increases monotonically with θ, and, as a consequence, Q decreases with concentration of salt for all values of θ.

The non-monotonic dependencies of Q on pH in Figures 11 and 14 may be explained by formation of ion pairs between fixed anions COO^- and mobile cations. At low pH values when concentration of H^+ ions is high, these pairs are formed between COO^- and H^+ ions. At high pH values, concentration of H^+ ions is small, but concentration of Na^+ ions is high (due to dissolution of NaOH), and ion pairs are formed between COO^- and Na^+ ions. In both cases, most functional groups attached to polymer chains remain neutral, which implies that Coulomb forces between bound charges are small, and the equilibrium degree of swelling is low. When pH of a bath is close to 7, concentrations of mobile cations are small, all functional groups are charged, and electrostatic repulsion between these groups induces a pronounced swelling of a gel.

V. CONCLUSIONS

A model is developed for the elastic response of and diffusion of solvent and solute through an anionic gel under swelling. A PE gel is treated as a three-phase continuum composed of a solid phase (an equivalent polymer network), solvent (water), and solute (mobile ions). Transport of solvent and solute is thought of as their diffusion accelerated by an electric field formed by mobile ions and bound charges and accompanied by chemical reactions (self-ionization of water molecules, dissociation of functional groups attached to polymer chains, and formation of ion pairs between bound charges and mobile counter-ions). Constitutive equations are derived by means of the free energy imbalance inequality for an arbitrary three-dimensional deformation with finite strains.

Unlike previous studies, both ionic pressure and electrostatic repulsion of bound charges are taken into account in the analysis of swelling of PE gels. The reference (stress-free) state of polymer chains is presumed to differ from the initial state of a dry undeformed gel. To account for electrostatic repulsion of bound charges in a tractable way, the coefficient of volume expansion of the equivalent network is treated as a linear function of degree of ionization of chains. A decay in water uptake by a PE gel with ionic strength of solution is explained by formation of electrically neutral ion-pairs between bound anions and mobile cations. A new version of the Henderson–Hasselbach equation is derived to describe this phenomenon.

An advantage of the constitutive model is that it treats the effects of pH and concentration of salt on swelling of a PE gel in a unified manner and does not require introduction of phenomenological relations to describe evolution of the dissociation constant[36–38] and the Flory–Huggins parameter[22,23] with ionic strength of solution.

The model is applied to study equilibrium swelling of poly(acrylic acid) gel, poly(acrylamide-co-sodium acrylate) gel, and DMAA–AMPS, NIPA–MAc copolymer gels with various molar fractions φ of ionic components. Analysis of experimental data leads to the following conclusions: (i) constitutive equations with the same material constants describe correctly the effects of pH and ionic strength on equilibrium

water uptake (Figures 1 and 2), (ii) when adjustable parameters are found by matching a swelling diagram in the entire interval of pH, the model predicts correctly evolution of degree of swelling with ionic strength (Figures 14 and 15), (iii) material parameters in the governing equations change consistently with concentration of PE component in copolymer gels (Figures 7 and 12), (iv) constraints imposed on deformation of a gel induce a severe decay in degree of swelling (Figure 10), (v) in accord with experimental data, equilibrium water uptake depends non-monotonically on ionic strength of solution under constrained swelling (Figure 3).

ACKNOWLEDGMENTS

Financial support by the EU Commission through FP-7 Project Evolution–314744 is gratefully acknowledged. The authors are thankful to the anonymous reviewers for valuable remarks and suggestions.

APPENDIX A: DERIVATIVE OF FREE ENERGY DENSITY

Substitution of Eqs. (31) and (54)–(58) into Eq. (53) implies that

$$\begin{aligned}\Psi = {}& \mu^0 C + k_B T C\Big(\ln\frac{Cv}{1+Cv} + \frac{\chi}{1+Cv}\Big) + \mu^0_{H^+} C_{H^+} \\ & + k_B T C_{H^+}\Big(\ln\frac{C_{H^+}}{C} - 1\Big) + \mu^0_{Na^+} C_{Na^+} \\ & + k_B T C_{Na^+}\Big(\ln\frac{C_{Na^+}}{C} - 1\Big) + \mu^0_{OH^-} C_{OH^-} \\ & + k_B T C_{OH^-}\Big(\ln\frac{C_{OH^-}}{C} - 1\Big) \\ & + \mu^0_{Cl^-} C_{Cl^-} + k_B T C_{Cl^-}\Big(\ln\frac{C_{Cl^-}}{C} - 1\Big) + W + W_{el} \\ & + k_B T C_b\Big[\beta_H \ln\beta_H + \beta_{Na}\ln\beta_{Na} \\ & + (1-\beta_H-\beta_{Na})\ln(1-\beta_H-\beta_{Na})\Big]. \end{aligned} \tag{A1}$$

The derivative of Eq. (55) with respect to time reads

$$\dot W = W_{,1}\dot J_{e1} + W_{,2}\dot J_{e2} + W_{,3}\dot J_{e1} + W_{,\alpha}\dot\alpha + W_{,f}\dot f,$$

where

$$W_{,m} = \frac{\partial W}{\partial J_{em}}, \qquad W_{,\alpha} = \frac{\partial W}{\partial \alpha}, \qquad W_{,f} = \frac{\partial W}{\partial f}.$$

Insertion of Eq. (52) into this equality yields

$$\dot W = 2\mathbf{K}_{mech} : \mathbf{D} + W_{,\alpha}\dot\alpha - \Big(\frac{2K}{3f} - W_{,f}\Big)\dot f, \tag{A2}$$

where

$$\begin{aligned}\mathbf{K}_{mech} &= W_{,1}\mathbf{B}_e - J_{e3}W_{,2}\mathbf{B}_e^{-1} + (J_{e2}W_{,2} + J_{e3}W_{,3})\mathbf{I}, \\ K &= J_{e1}W_{,1} + 2J_{e2}W_{,2} + 3J_{e3}W_{,3}.\end{aligned} \tag{A3}$$

Differentiation of Eq. (31) with respect to time implies that

$$\dot W_{el} = \frac{1}{2\epsilon J}\Big(2\mathbf{H}\cdot\mathbf{C}\cdot\dot{\mathbf{H}} + \mathbf{H}\cdot\dot{\mathbf{C}}\cdot\mathbf{H} - \frac{\dot J}{J}\mathbf{H}\cdot\mathbf{C}\cdot\mathbf{H}\Big).$$

This relation together with Eq. (29) results in

$$\dot W_{el} = \mathbf{E}\cdot\dot{\mathbf{H}} + \frac{1}{2\epsilon J}\Big(\mathbf{H}\cdot\dot{\mathbf{C}}\cdot\mathbf{H} - \frac{\dot J}{J}\mathbf{H}\cdot\mathbf{C}\cdot\mathbf{H}\Big). \tag{A4}$$

It follows from Eqs. (13), (49), and (50) that

$$\dot{\mathbf{C}} = 2\mathbf{F}^\top\cdot\mathbf{D}\cdot\mathbf{F}.$$

Combination of this equality with Eq. (29) yields

$$\begin{aligned}\frac{1}{2\epsilon J}\mathbf{H}\cdot\dot{\mathbf{C}}\cdot\mathbf{H} &= \frac{1}{\epsilon J}\mathbf{H}\cdot\mathbf{F}^\top\cdot\mathbf{D}\cdot\mathbf{F}\cdot\mathbf{H} \\ &= \frac{J}{\epsilon}\mathbf{h}\cdot\mathbf{D}\cdot\mathbf{h} = \frac{J}{\epsilon}(\mathbf{h}\otimes\mathbf{h}) : \mathbf{D},\end{aligned} \tag{A5}$$

where $\otimes$ stands for tensor product. Keeping in mind that

$$\dot J = J\mathbf{I} : \mathbf{D} \tag{A6}$$

and utilizing Eq. (13), we conclude that

$$\frac{\dot J}{2\epsilon J^2}\mathbf{H}\cdot\mathbf{C}\cdot\mathbf{H} = \frac{1}{2\epsilon J}\mathbf{H}\cdot\mathbf{F}^\top\cdot\mathbf{F}\cdot\mathbf{H}(\mathbf{I}:\mathbf{D}) = \frac{J}{2\epsilon}(\mathbf{h}\cdot\mathbf{h})\mathbf{I} : \mathbf{D}. \tag{A7}$$

Substitution of Eqs. (A5) and (A7) into Eq. (A4) implies that

$$\dot W_{el} = \mathbf{E}\cdot\dot{\mathbf{H}} + 2\mathbf{K}_{el} : \mathbf{D}, \tag{A8}$$

where

$$\mathbf{K}_{el} = \frac{J}{2\epsilon}\Big[(\mathbf{h}\otimes\mathbf{h}) - \frac{1}{2}(\mathbf{h}\cdot\mathbf{h})\mathbf{I}\Big]. \tag{A9}$$

Differentiating Eq. (A1) with respect to time and using Eqs. (10), (A2), and (A8), we arrive at Eq. (63) with

$$\begin{aligned}\Theta_C &= \mu^0 + k_B T\Big[\ln\frac{Cv}{1+Cv} + \frac{1}{1+Cv} + \frac{\chi}{(1+Cv)^2} \\ &\quad - \frac{C_{H^+}+C_{Na^+}+C_{OH^-}+C_{Cl^-}}{C}\Big], \\ \Theta_{H^+} &= \mu^0_{H^+} + k_B T\ln\frac{C_{H^+}}{C}, \\ \Theta_{Na^+} &= \mu^0_{Na^+} + k_B T\ln\frac{C_{Na^+}}{C}, \\ \Theta_{OH^-} &= \mu^0_{OH^-} + k_B T\ln\frac{C_{OH^-}}{C}, \\ \Theta_{Cl^-} &= \mu^0_{Cl^-} + k_B T\ln\frac{C_{Cl^-}}{C}, \\ \Theta_{\beta_H} &= k_B T C_b\ln\frac{\beta_H}{1-\beta_H-\beta_{Na}}, \\ \Theta_{\beta_{Na}} &= k_B T C_b\ln\frac{\beta_{Na}}{1-\beta_H-\beta_{Na}}.\end{aligned} \tag{A10}$$

APPENDIX B: DONNAN EQUILIBRIUM CONDITIONS

Insertion of Eq. (70) into Eq. (88) implies that

$$\begin{aligned}\ln\frac{C_{H^+}}{C} &= \ln\frac{\bar c_{H^+}}{\bar c} - \frac{e}{k_B T}(\Phi-\bar\Phi), \\ \ln\frac{C_{Na^+}}{C} &= \ln\frac{\bar c_{Na^+}}{\bar c} - \frac{e}{k_B T}(\Phi-\bar\Phi), \\ \ln\frac{C_{OH^-}}{C} &= \ln\frac{\bar c_{OH^-}}{\bar c} + \frac{e}{k_B T}(\Phi-\bar\Phi), \\ \ln\frac{C_{Cl^-}}{C} &= \ln\frac{\bar c_{Cl^-}}{\bar c} + \frac{e}{k_B T}(\Phi-\bar\Phi),\end{aligned} \tag{B1}$$

where concentrations of water molecules and mobile ions in the bath in the initial configuration are replaced with their

concentrations in the actual configuration. It follows from Eq. (B1) that

$$\frac{C_{H^+}}{C}\frac{C_{OH^-}+C_{Cl^-}}{C}=\frac{\bar c_{H^+}}{\bar c}\frac{\bar c_{OH^-}+\bar c_{Cl^-}}{\bar c}, \tag{B2}$$

$$\frac{C_{H^+}+C_{Na^+}}{C}\frac{C_{OH^-}+C_{Cl^-}}{C}=\frac{\bar c_{H^+}+\bar c_{Na^+}}{\bar c}\frac{\bar c_{OH^-}+\bar c_{Cl^-}}{\bar c}. \tag{B3}$$

The electro-neutrality conditions for the gel and bath read

$$C_{OH^-}+C_{Cl^-}=C_{H^+}+C_{Na^+}-\alpha C_b, \tag{B4}$$

$$\bar c_{OH^-}+\bar c_{Cl^-}=\bar c_{H^+}+\bar c_{Na^+}. \tag{B5}$$

Inserting Eq. (B5) into Eq. (B3) and using Eqs. (2), (11), and (12), we find that

$$\frac{C_{H^+}+C_{Na^+}}{C}\frac{C_{OH^-}+C_{Cl^-}}{C}=\frac{1}{\kappa^2}(10^{-pH}+\theta)^2. \tag{B6}$$

Combination of Eqs. (B4) and (B6) results in

$$X\Big(X-\alpha\frac{C_b}{C}\Big)=\frac{1}{\kappa^2}(10^{-pH}+\theta)^2, \tag{B7}$$

where X is determined by Eq. (92). It follows from Equations (2) and (11), (12), (B2), (B4), and (B5) that

$$X_1\Big(X-\alpha\frac{C_b}{C}\Big)=\frac{1}{\kappa^2}10^{-pH}(10^{-pH}+\theta), \tag{B8}$$

where

$$X_1=\frac{C_{H^+}}{C}. \tag{B9}$$

Eqs. (B7), (B8) imply that

$$X_1=\frac{10^{-pH}}{10^{-pH}+\theta}X. \tag{B10}$$

Substitution of Eqs. (92) and (B9) into Eq. (76) yields

$$\alpha=K_a'\Big[K_a'+X_1+R(X-X_1)\Big]^{-1}. \tag{B11}$$

Combination of Eqs. (B10) and (B11) results in Eq. (90).

Inserting Eqs. (92) and (B4) into Eq. (70), we calculate chemical potential of water molecules in the gel

$$\mu=\mu^0+k_BT\Big[\ln\frac{Cv}{1+Cv}+\frac{1}{1+Cv}+\frac{\chi}{(1+Cv)^2}+\frac{\Pi v}{k_BT}-\Big(2X-\alpha\frac{C_b}{C}\Big)\Big]. \tag{B12}$$

Chemical potential of water molecules in the bath is given by Eq. (70) where the first four terms in the square brackets (which describe interaction between the polymer network and solvent) are disregarded

$$\bar\mu=\mu^0-k_BT\frac{\bar c_{H^+}+\bar c_{Na^+}+\bar c_{OH^-}+\bar c_{Cl^-}}{\bar c}.$$

Applying Eqs. (2), (11), (12), and (B5), we transform this expression as follows:

$$\bar\mu=\mu^0-\frac{2k_BT}{\kappa}(10^{-pH}+\theta). \tag{B13}$$

Substitution of Eqs. (B12) and (B13) into Eq. (88) implies that

$$\ln\frac{Cv}{1+Cv}+\frac{1}{1+Cv}+\frac{\chi}{(1+Cv)^2}+\frac{\Pi v}{k_BT}+\alpha\frac{C_b}{C}-2\Big[X-\frac{1}{\kappa}(10^{-pH}+\theta)\Big]=0. \tag{B14}$$

It follows from Eq. (B7) that

$$\Big(X-\frac{1}{\kappa}(10^{-pH}+\theta)\Big)\Big(X+\frac{1}{\kappa}(10^{-pH}+\theta)\Big)=\frac{\alpha C_b}{C}X,$$

which means that

$$\Big(X-\frac{1}{\kappa}(10^{-pH}+\theta)\Big)=\frac{\alpha C_b}{C}X\Big(X+\frac{1}{\kappa}(10^{-pH}+\theta)\Big)^{-1}. \tag{B15}$$

Combination of Eqs. (B14) and (B15) yields

$$\ln\frac{Cv}{1+Cv}+\frac{1}{1+Cv}+\frac{\chi}{(1+Cv)^2}+\frac{\Pi v}{k_BT}-X\Big(\alpha\frac{C_b}{C}\Big)^2\Big(X+\frac{1}{\kappa}(10^{-pH}+\theta)\Big)^{-2}=0. \tag{B16}$$

Equations (89) and (91) follow from Eqs. (92), (B7), and (B16).

[1] S. Van Vlierberghe, P. Dubruel, and E. Schacht, Biomacromolecules **12**, 1387 (2011).
[2] S.-K. Ahn, R. M. Kasi, S.-C. Kim, N. Sharma, and Y. Zhou, Soft Matter **4**, 1151 (2008).
[3] E. M. White, J. Yatvin, J. B. Grubbs, J. A. Bilbrey, and J. Locklin, J. Polym. Sci., Part B: Polym. Phys. **51**, 1084 (2013).
[4] A. Doring, W. Birnbaum, and D. Kuckling, Chem. Soc. Rev. **42**, 7391 (2013).
[5] S. E. Kudaibergenov, N. Nuraje, and V. V. Khutoryanskiy, Soft Matter **8**, 9302 (2012).
[6] K. Deligkaris, T. S. Tadele, W. Olthuis, and A. van den Berg, Sens. Actuators, B **147**, 765 (2010).
[7] R. Messing and A. M. Schmidt, Polym. Chem. **2**, 18 (2011).
[8] D. Buenger, F. Topuz, and J. Groll, Prog. Polym. Sci. **37**, 1678 (2012).
[9] C. Alvarez-Lorenzo and A. Concheiro, Chem. Commun. **50**, 7743 (2014).
[10] E. Kokufuta, Langmuir **21**, 10004 (2005).
[11] S. Mafe, J. A. Manzanares, A. E. English, and T. Tanaka, Phys. Rev. Lett. **79**, 3086 (1997).
[12] A. V. Dobrynin and M. Rubinstein, Prog. Polym. Sci. **30**, 1049 (2005).
[13] G. S. Longo, M. Olvera de la Cruz, and I. Szleifer, Macromolecules **44**, 147 (2011).
[14] J. Hua, M. K. Mitra, and M. Muthukumar, J. Chem. Phys. **136**, 134901 (2012).
[15] A. Fernandez-Nieves, A. Fernandez-Barbero, and F. J. de las Nieves, J. Chem. Phys. **115**, 7644 (2001).
[16] G. S. Manning, J. Chem. Phys. **51**, 924 (1969).
[17] M. Satoh, J. Komiyama, and T. Iijima, Macromolecules **18**, 1195 (1985).
[18] M. Muthukumar, J. Chem. Phys. **120**, 9343 (2004).
[19] G. M. Eichenbaum, P. F. Kiser, S. A. Simon, and D. Needham, Macromolecules **31**, 5084 (1998).
[20] G. M. Eichenbaum, P. F. Kiser, A. V. Dobrynin, S. A. Simon, and D. Needham, Macromolecules **32**, 4867 (1999).
[21] E. Y. Kramarenko, A. R. Khokhlov, and K. Yoshikawa, Macromol. Theory Simul. **9**, 249 (2000).
[22] W. Cai and R. B. Gupta, J. Appl. Polym. Sci. **88**, 2032 (2003).
[23] H. Lu and S. Du, Polym. Chem. **5**, 1155 (2014).
[24] R. Marcombe, S. Cai, W. Hong, X. Zhao, Y. Lapusta, and Z. Suo, Soft Matter **6**, 784 (2010).
[25] M. Quesada-Perez, J. A. Maroto-Centeno, J. Forcada, and R. Hidalgo-Alvarez, Soft Matter **7**, 10536 (2011).
[26] L. Feng, Y. Jia, X. Chen, X. Li, and L. An, J. Chem. Phys. **133**, 114904 (2010).
[27] W. Hong, X. Zhao, and Z. Suo, J. Mech. Phys. Solids **58**, 558 (2010).
[28] T. Y. Ng, H. Li, and Y. K. Yew, Int. J. Solids Struct. **47**, 614 (2010).
[29] J. P. Keener, S. Sircar, and A. L. Fogelson, Phys. Rev. E **83**, 041802 (2011).
[30] T. Wallmersperger, K. Keller, B. Kroplin, M. Gunther, and G. Gerlach, Colloid Polym. Sci. **289**, 535 (2011).
[31] J. C. Kurnia, E. Birgersson, and A. S. Mujumdar, Polymer **53**, 613 (2012).

[32]Y. Mori, H. Chen, C. Micek, and M.-C. Calderer, SIAM J. Appl. Math. **73**, 104 (2013).
[33]J. Li, Z. Suo, and J. J. Vlassak, Soft Matter **10**, 2582 (2014).
[34]H. Yan and B. Jin, Eur. Phys. J. E **36**, 27 (2013).
[35]H. Yan, B. Jin, S. Gao, and L. Chen, Int. J. Solids Struct. **51**, 4149 (2014).
[36]F. Lai and H. Li, Soft Matter **6**, 311 (2010).
[37]F. Lai, H. Li, and R. Luo, Int. J. Solids Struct. **47**, 3141 (2010).
[38]F. Lai and H. Li, Mech. Mater. **43**, 287 (2011).
[39]S. Sircar, J. P. Keener, and A. L. Fogelson, J. Chem. Phys. **138**, 014901 (2013).
[40]P. Nardinocchi, M. Pezzula, and L. Placidi, J. Intell. Mater. Syst. Struct. **22**, 1887 (2011).
[41]R. Andreu, J. J. Calvente, W. R. Fawcett, and M. Molero, Langmuir **13**, 5189 (1997).
[42]R. Bustamante, A. Dorfmann, and R. W. Ogden, Int. J. Eng. Sci. **47**, 1131 (2009).
[43]A. R. Khokhlov, J. Phys. A **13**, 979 (1980).
[44]K. Kamran, M. van Soestbergen, H. P. Huinink, and L. Pel, Electrochim. Acta **78**, 229 (2012).
[45]J. Ricka and T. Tanaka, Macromolecules **17**, 2916 (1984).
[46]A. D. Drozdov, Int. J. Appl. Mech. **6**, 1450023 (2014).
[47]E. Fried and S. Seller, J. Mech. Phys. Solids **52**, 1671 (2004).
[48]A. D. Drozdov and J. deC. Christiansen, Int. J. Solids Struct. **50**, 1494 (2013).
[49]A. D. Drozdov and J. deC. Christiansen, Int. J. Solids Struct. **50**, 3570 (2013).
[50]Q. Liu, A. Robisson, Y. Lou, and Z. Suo, J. Appl. Phys. **114**, 064901 (2013).
[51]L. Zhang, M. W. Spears, and L. A. Lyon, Langmuir **30**, 7628 (2014).
[52]D. Capriles-Gonzalez, B. Sierra-Martin, A. Fernandez-Nieves, and A. Fernandez-Barbero, J. Phys. Chem. B **112**, 12195 (2008).
[53]K. Takada, K. Ito, and A. Yuchi, Sens. Actuators, B **142**, 377 (2009).
[54]H.-C. Chiu, Y.-F. Lin, and S.-H. Hung, Macromolecules **35**, 5235 (2002).
[55]T. Wu, P. Gong, I. Szleifer, P. Vlcek, V. Syubr, and J. Genzer, Macromolecules **40**, 8756 (2007).
[56]P. Gong, T. Wu, J. Genzer, and I. Szleifer, Macromolecules **40**, 8765 (2007).
[57]R. Israels, F. A. M. Leermakers, and G. J. Fleer, Macromolecules **27**, 3087 (1994).
[58]G. S. Longo, M. Olvera de la Cruz, and I. Szleifer, J. Chem. Phys. **141**, 124909 (2014).
[59]S. Naficy, J. M. Razal, P. G. Whitten, G. G. Wallace, and G. M. Spinks, J. Polym. Sci., Part B: Polym. Phys. **50**, 423 (2012).
[60]X. Liu, Z. Tong, and O. Hu, Macromolecules **28**, 3813 (1995).
[61]A. M. Atta, H. S. Ismail, H. M. Mohamed, and Z. M. Mohamed, J. Appl. Polym. Sci. **122**, 999 (2011).
[62]A. M. Atta, H. S. Ismail, and A. M. Elsaaed, J. Appl. Polym. Sci. **123**, 2500 (2011).
[63]A. El-Hag Ali, J. Appl. Polym. Sci. **123**, 763 (2012).
[64]S. Zhou and B. Chu, J. Phys. Chem. B **102**, 1364 (1998).
[65]S. Fisher and R. Kunin, J. Phys. Chem. **60**, 1030 (1956).
[66]E. Vasheghani-Farahani, J. H. Vera, D. G. Cooper, and M. E. Weber, Ind. Eng. Chem. Res. **29**, 554 (1990).